STATE OF OREGON
DEPARTMENT OF GEOLOGY AND MINERAL INDUSTRIES
1005 State Office Building, Portland, Oregon 97201

OPEN-FILE REPORT O-81-9

SEISMIC AND VOLCANIC HAZARD EVALUATION OF THE MOUNT ST. HELENS AREA, WASHINGTON RELATIVE TO THE TROJAN NUCLEAR SITE, OREGON

John D. Beaulieu
Deputy State Geologist

Norman V. Peterson
Geologist

Conducted in conformance with ORS 516.030

Funded by Oregon Department of Energy

September 1981

CONTENTS

LIST OF FIGURES

LIST OF TABLES

1.0 INTRODUCTION

In spring 1978 the Oregon Department of Geology and Mineral Industries was requested by the Oregon Department of Energy to review the adequacy of the siting considerations of the Trojan Nuclear Power Plant in light of possible new information developed subsequent to original siting review. It was concluded that there was no information available to necessitate reconsiderations of the siting decision. The future need to reconsider that conclusion in view of possible future developments was noted.

On May 18, 1980, Mount St. Helens, situated 35 miles east of the facility (Figure 1b) erupted causing renewed interest in volcanic hazard potential as a siting consideration. Additionally, ongoing study of seismic activity has led to the concept of a seismic zone representing a possible fault or faults of 100 km length passing within approximately 30 miles of the facility.

On May 18, 1981, the Oregon Department of Geology and Mineral Industries was requested by the Oregon Department of Energy to conduct an investigation consisting of the following elements:

Seismic: With respect to the suspected faults to review existing data and conclusions, to document its own conclusions regarding the possible existence, location, and capability of the fault, to determine likely attenuation of associated ground motion, and to bound the characteristics of the fault as a means of recommended further work that is warranted, if any, with respect to Trojan.

Volcanic: With respect to existing estimates of the future behavior of Mount St. Helens to assess geologic assumptions used to characterize lateral blasts, ash falls, pyroclastic flows, mudflows, and floods; to document its own conclusions regarding the validity of existing estimates; to provide bounds for expected behavior where appropriate, and to identify additional further work that is warranted, if any, with respect to Trojan.

This study is a systematic and comprehensive inquiry into existing assumptions, data, and conclusions which bear directly or indirectly on the formulation of a credible response to the request of the Oregon Department of Energy.

Throughout the investigation, assumptions are clearly stated; data are clearly evaluated and referenced as to source; and conclusions are carefully stated. The discussions are technical by necessity, and more general introductions and summaries of major sections are provided to assist the reader.

We have attempted to avoid personal bias through application of the scientific method. The potential for actual bias of data owing to finite limits of observation is addressed through critical evaluation of data sets, appeal to multiple analytical techniques, cross checking of conclusions, and multiple interpretations of critical features or parameters where possible.

In the interpretation of seismic potential, a conservative estimate of the presumed fault is analyzed using six source parameter equations, an approximation of seismic moment, and a consideration of recurrence frequency as suggested by limited historic records. The resulting estimate of maximum possible earthquake is interpreted in terms of existing attenuation models to yield a seismic response spectrum at the site. This, then, is compared with the ground motion data used in the original design of the Trojan facility.

Volcanic hazards analyzed include lateral blast, ash fall, pyroclastic flow, mudflow, and floods. For each volcanic hazard the magnitude of the maximum credible event is determined by a knowledge of the geologic and historic record at and surrounding Mount St. Helens, an understanding of analogous volcanoes and the mechanics of the processes in question, and a judgment of the adequacy of available data. Where data are limited this shortcoming is offset by increased conservatism in this review.

Prehistoric andesite and basalt lava flows have been erupted from the upper flanks of Mount St. Helens. However, they are few in number and rarely do they extend beyond the break in slope at the foot of the mountain. Therefore, they are not considered further in this report.

2.0 REGIONAL GEOLOGIC SETTING

2.1 General

The tectonism and geology of western North America are viewed here in the context of plate tectonic theory, which holds that the North American Plate is drifting westward relative to the West Pacific Plate and has actually overridden it along a zone of subduction (Atwater, 1970). Development of this theory arises from a wide variety of scientific data involving both onshore and offshore areas. Recent syntheses are proceeding toward coherent explanations of the deformations we observe in place and time throughout the western North American Plate. Appeal to this theory is prudent for full analysis of the specific seismic activity addressed by this study.

The plate tectonic models understandably contain a range of uncertainty, yet are of general benefit in view of common agreement on major points. In particular, attempts at developing a regional synthesis of plate tectonic geologic processes are of value in interpreting specific geologic events or features. They place rational constraints on speculation on the one hand while guiding rational extrapolations of limited data on the other.

2.2 Plate Tectonic Boundaries in the Northwest United States

The major plate tectonic boundaries getween the North American Plate and the West Pacific Plate include the Queen Charlotte Island Fault along the west coast of Canada and the San Andreas Fault of California. Both are simple faults of the transform type and exhibit ongoing right lateral displacement. Vector calculations of gross plate movements suggest rates of displacement of 5-6 cm per year (Coney, 1978; Silver, 1971) whereas geodetic measurements and regional geologic mapping indicate displacements of slightly more than half that amount (Coney, 1978; Smith, 1977).

In the Pacific Northwest, between Vancouver Island and Cape Mendocino (Figure 1a) several small spreading centers off the coast separate the Queen Charlotte Fairweather Fault and the San Andreas Fault and yield several small plates collectively referred to here as the Farallon Plate (Juan de Fuca Plate). From south to north are located the eastern end of Mendocino (or Gorda) Escarpment, Gorda Ridge, the Blanco Fracture Zone, Juan de Fuca Ridge, Sovanco Fracture Zone, Explorer Ridge, and the Queen Charlotte-Fairweather Fault System.

Silver (1978), Riddihough (1977), Davis (1977), and Carlson (1976) among others conclude that despite lack of an inclined Benioff (seismic) zone beneath western Washington and Oregon, eastward subduction of the Farallon Plate beneath North America is probably occurring. More recently, Crosson (1980) has presented seismic focal data that strongly suggests the existence of a shallow east-dipping Benioff zone beneath the western and central parts of the Puget Trough at the latitude of the Olympic Peninsula.

Other features supportive of Quaternary subduction beneath the continent include the compressive deformation of late Pleistocene sediments along the base of the Oregon-Washington continental slope and the nature of the deep (60-70 km) Puget Sound-Gulf Islands earthquakes as discussed below. Further, heat flow measurements define a belt of low heat flow inland from the coast changing to high heat flow near the volcanic arc (Cascades). Gravity anomalies over the margin display the linear "high and low" pattern characteristic of active plate margins. Continued volcanism in the Cascades, although of a lower rate than sometimes in the past, also supports continuing movement on the subduction zone.

The general lack of historic seismicity along the subduction zone is anomalous but can be attributed to a variety of features particular to the Farallon (Juan de Fuca) Plate. These include: (1) its relative thinness, which may not allow large scale accumulation of stress, (2) its relative youth and its thick insulating cover of sediments, both of which may result in maintenance of higher temperatures and higher plasticity, and (3) a relatively low rate of subduction which may favor aseismic (rather than seismic) creep.

The relative direction of convergence between the North American and Farallon (Juan de Fuca) Plates is unclear. Estimates are based on the movement vectors of various plates as shown by the example in Figure 1a. There the vectors are plotted relative to north with information derived from pertinent geologic features so that Pn is the movement of the Pacific Plate relative to the North American Plate (using San Andreas Fault as a reference), Fp is the movement of the Farallon Plate relative to the Pacific Plate (using the Juan de Fuca Ridge as a reference) and Nf is the movement of the North American Plate relative to the Farallon Plate (defined by connecting the other two vectors). Rates of movement are 6.0 cm/yr for Pn and 5.8 cm/yr for Fp. Nf here is indicative of underthrusting at an angle of N. 38^{o} E. at a rate of 3 cm/yr oblique to the subduction zone. The obliqueness of the subduction may impose a right lateral component of strain on the overriding North American Plate (Davis, 1981).

The specific angle of convergence may be significant in understanding major structures in the North American Plate, such as the possible one (Section 2.3) under consideration here. In addition to the above example of oblique subduction (N. 38^{o} E.) a suggested angle of N. 50^{o} E. is proposed by Riddihough (1977). Neither angle is totally consistent with the postulated orientation (N. 20^{o} W.) of the Mount St. Helens Seismic Zone of Weaver and Smith (1981). This inconsistency may be resolved in the future with: (1) more precise vectoral solutions, (2) refined definition of the Mount St. Helens Seismic Zone and its orientation, (3) integration of knowledge of possible deep crustal preexisting zones of weakness, or (4) better understanding of the overall geology of the study area.

Tentative conclusions can be drawn about the specific geometry of the subducting plate. Seismic activity at depths greater than 20 km indicates east-west tension (Hill, 1978). The 1965 Seattle earthquake was produced along a north-south striking normal fault at a depth of 60 km. The faulting is

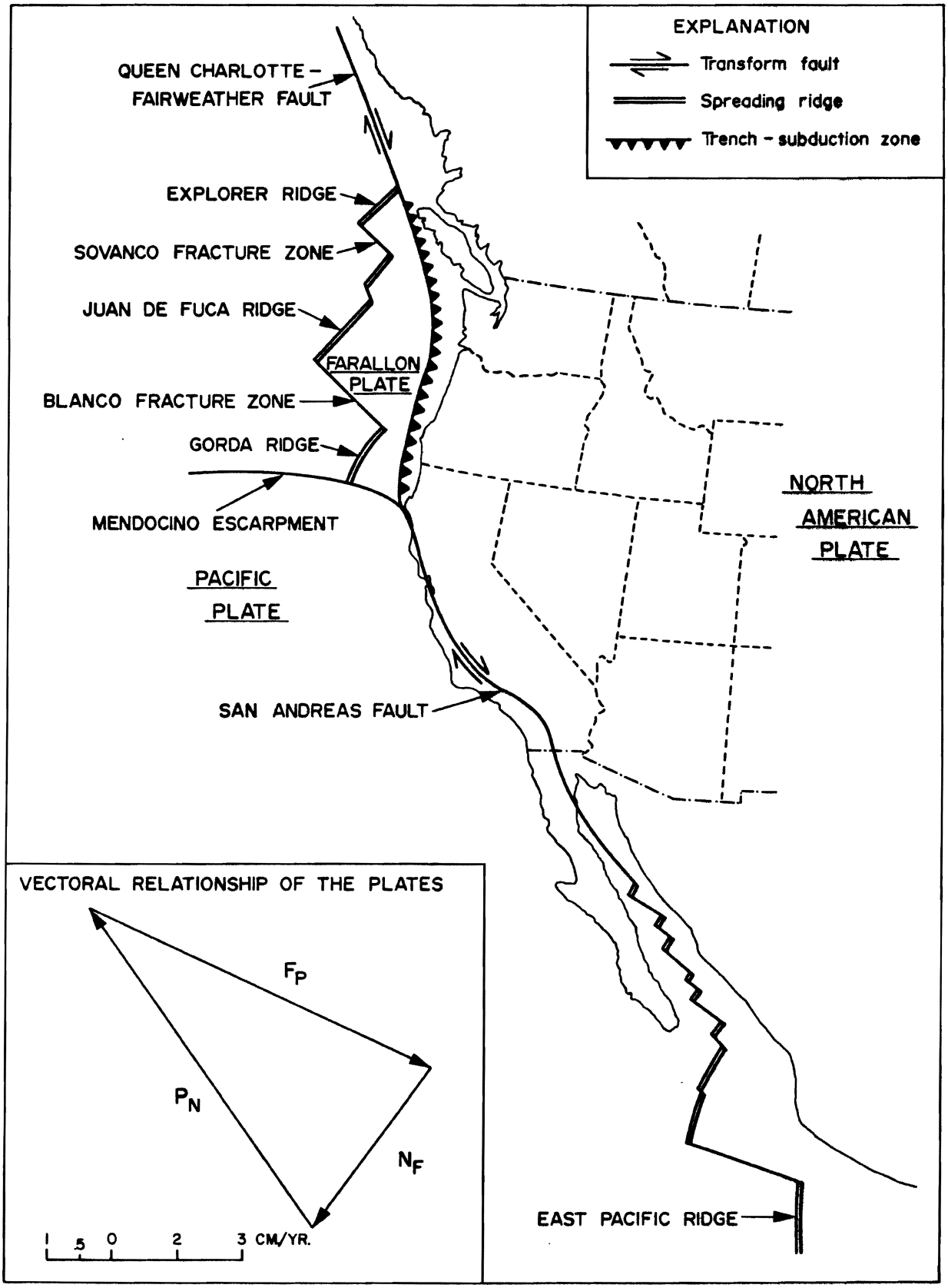

Figure 1a. Plate tectonic setting of Oregon and Washington.

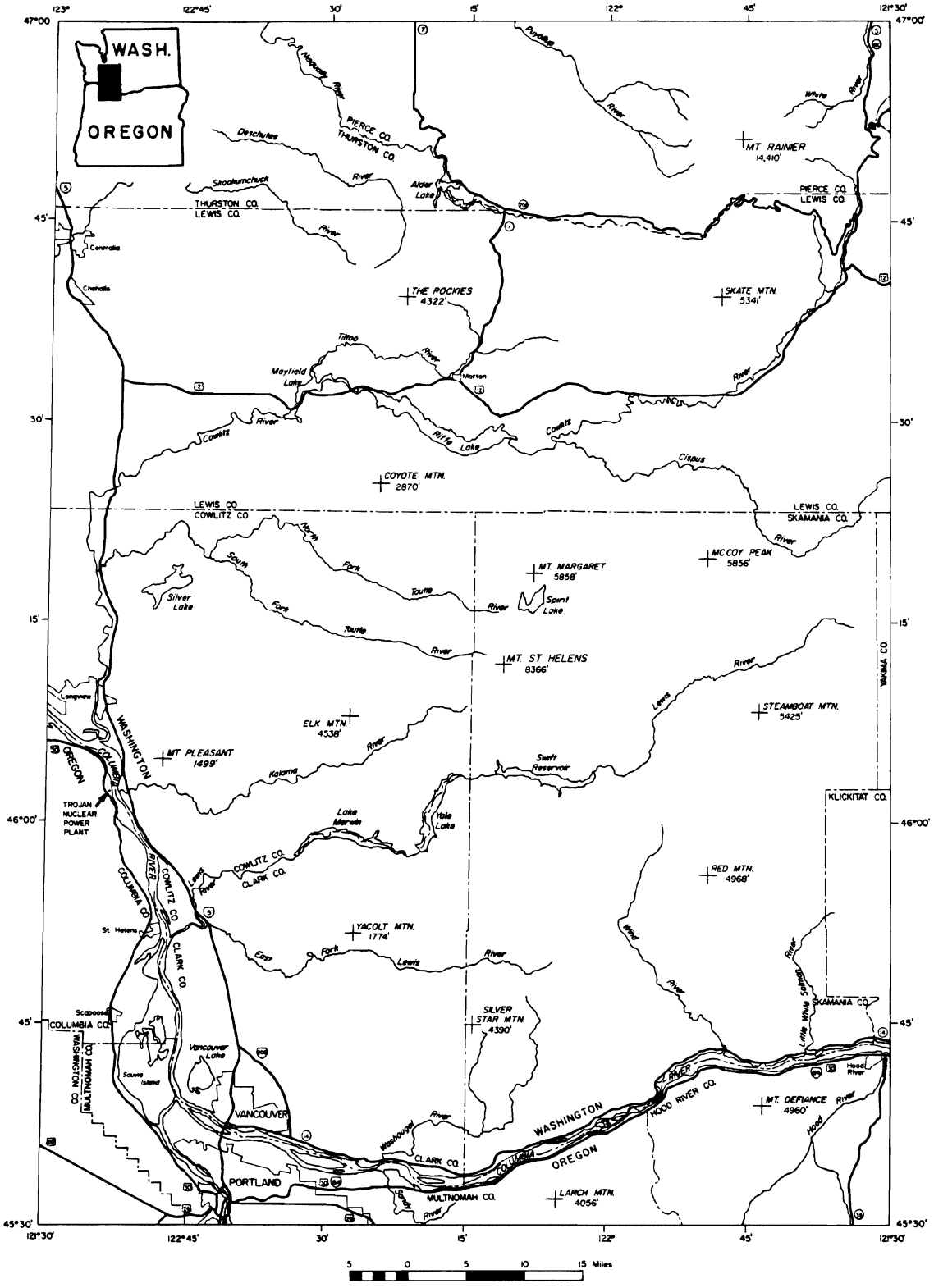

Fig. 1b. Location map of Mount St. Helens area.

attributed by Davis (1977) to tension on the upper part of the subducting plate in a region of abrupt steepening to the east. The depth of the 1965 Seattle quake suggests a 10^{o}-15^{o} dip of the subducting plate eastward from the base of the continental slope to the Puget Sound area. Farther to the east a 30^{o}-50^{o} dip is required to allow for the generation of magma for Quaternary Cascade volcanoes east of the Puget Trough. For the 1965 Seattle earthquake (longitude $122^{o}20'$W) Langston and Blum (1977) interpret an east dipping (70^{o}) low velocity zone at a depth of 41-56 km, a conclusion in general agreement with the subduction model.

Oblique subduction as described above allows for a variety of models of deformation in the northwestern United States. Conceivably northeast subduction of the lower plate (oblique to the margin of the upper plate) and northwesterly shear of the upper plate can accommodate the regional stress regime. The relative significance of the two mechanisms should reflect the degree of "locking" of the two plates. A "locked" situation would be seen in dominant northwest shear and inelastic permanent deformation of the upper plate; whereas, an unlocked situation would be seen in dominant seismic or aseismic creep along the subduction zone. Further, mechanical response to the oblique subduction may vary from time to time and from place to place.

The only major earthquakes which appear to be associated with the subduction zone occur beneath Puget Sound and Vancouver Island. There, the subducted plate appears to be under east-west tension at least in the upper parts. Decoupling of the plates in the zone of seismicity west of the Cascades can be postulated. Additional decoupling through aseismic means is possible elsewhere including regions beneath the Cascades. However, northwest shear along the Mount St. Helens Seismic Zone can be construed as evidence for a partially locked situation at present. From a geologic or seismologic standpoint it is not possible to provide a complete and final statement of the degree of "locking" or "unlocking" of the plates at this time.

In an analogous area of oblique subduction near New Zealand, plate locking and unlocking in a historic time frame is documented by Walcott (1978), who notes that final interpretations in complex areas of that type must consider seismic and aseismic subduction, lateral faulting in the upper plate, and permanent inelastic deformation of the upper plate.

2.3 The Mount St. Helens Seismic Zone

The Mount St. Helens seismic zone is defined generally as a north 20^{o} west trending band of seismic activity extending a maximum distance of 100 km from the Swift Reservoir on the south past Mount St. Helens to the vicinity of Alder Lake on the Nisqually River on the north. It is defined by Weaver and Smith (1981) on the basis of earthquakes of magnitude (Mc) $\geq$ 2.8 occurring between mid-1970 and February 15, 1981. All events occur at depths of 20 km or less. Right lateral fault plane solutions with vertical faults are available for some of the events.

Detailed seismic evaluation of post May 18, 1980 events suggests that the zone to the south of Mount St. Helens consists of more than one fault rather than a single fault (Weaver and others, 1981). Crosson (1972), using a broader data base with lower resolution in terms of locations, described the seismicity of western Washington as diffuse rather than as occurring in well-defined zones.

Conceptually, the Mount St. Helens Seismic Zone lies above the locus of relative steepening of the underlying subducting plate to the east. Also, in a regional kinematic model the seismic zone is favorably situated to accommodate right lateral shear over an obliquely subducting plate. The seismic zone is bounded to the north by the Puget Sound Province and possibly to the south by a sub-province of the Cascades characterized by relatively voluminous outpourings of basaltic to dacitic lava in an east-west extensional regime. Available gravity data (Gower, 1978) do not suggest continuation of the zone northward beneath the Puget Sound area. Thus, regional geologic considerations bound the length of the feature.

Available geologic maps are of the reconnaissance type and do not depict faulting of the type suggested by the seismic data as defined herein. Yet the extent and shallow depth of the seismic activity suggest the presence of one or more faults at the surface. Synoptic rational lineament maps of the area prepared in this study provide indirect indications of possible faults in the area as shown in Figures 2a, b, and c. A synoptic rational lineament map is a map of lineaments from relatively small scale (large area) imagery in which the kinds of lineaments to be plotted are objectively defined in advance. As noted in Figure 2b, northerly trending lineaments do not lend themselves to

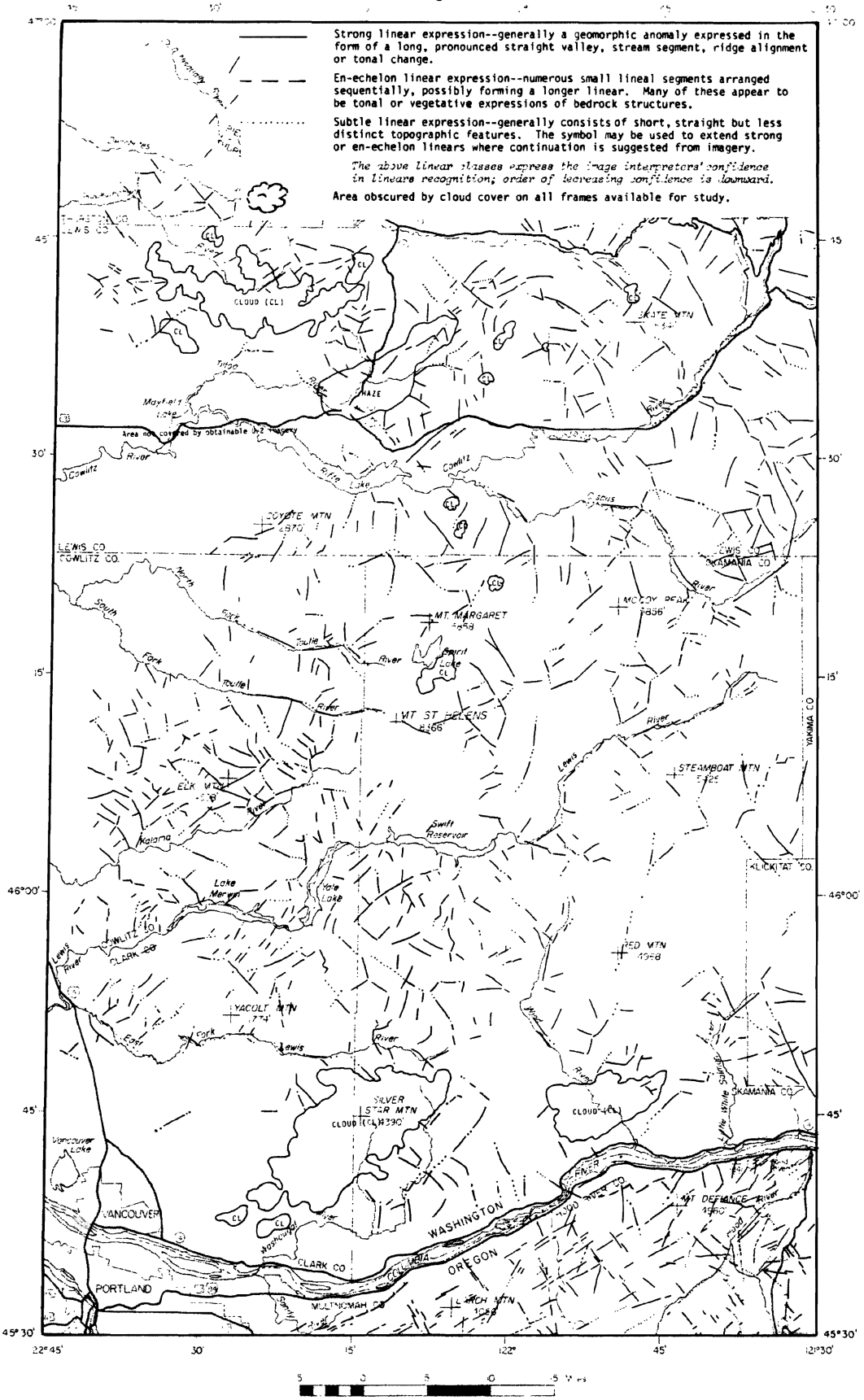

Figure 2a. Geologic lineaments of the Mount St. Helens area derived from high altitude (U-2) color infrared aerial photographs.

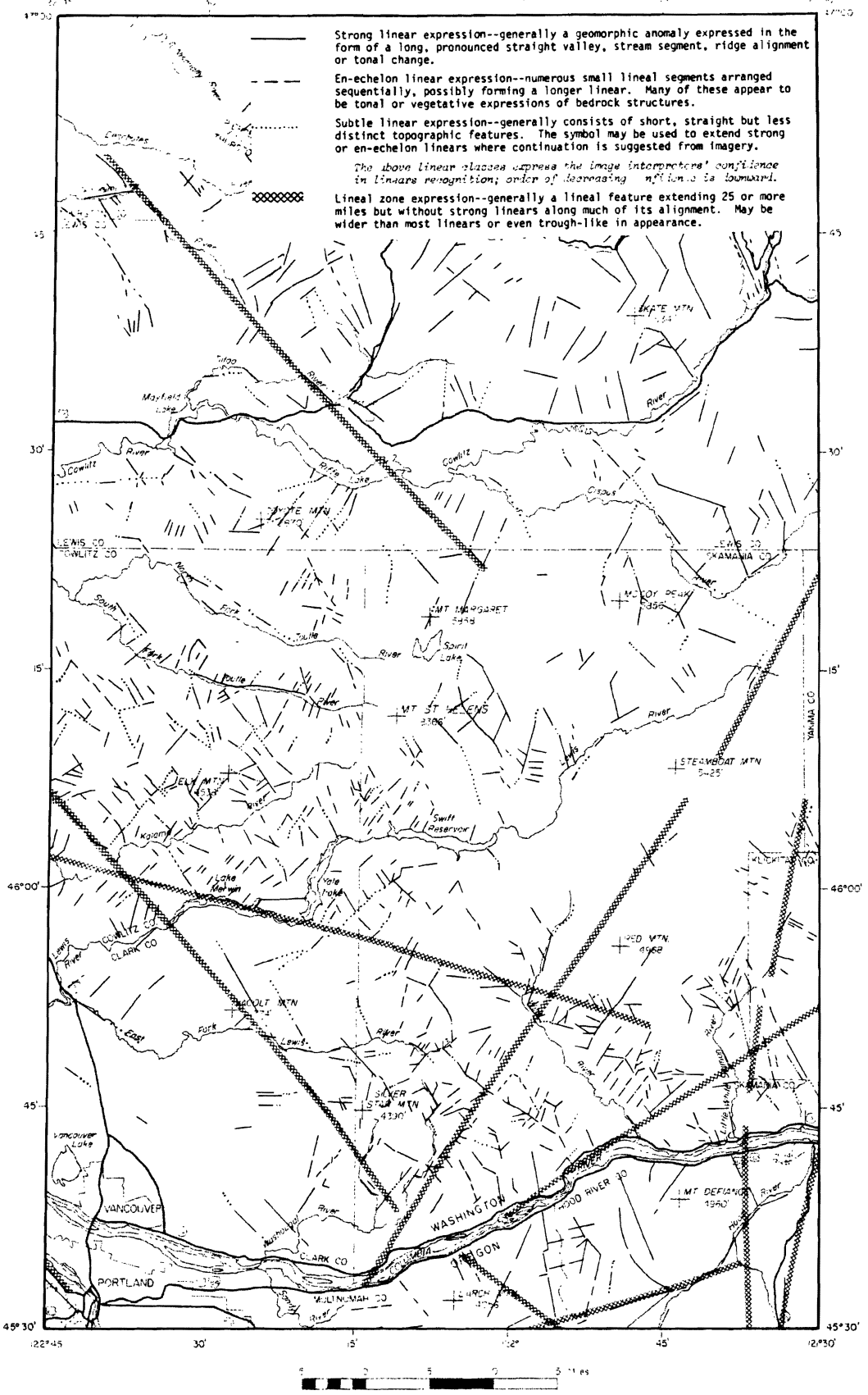

Figure 2b. Geologic lineaments of the Mount St. Helens area derived from side looking airborne radar (SLAR) mosaics.

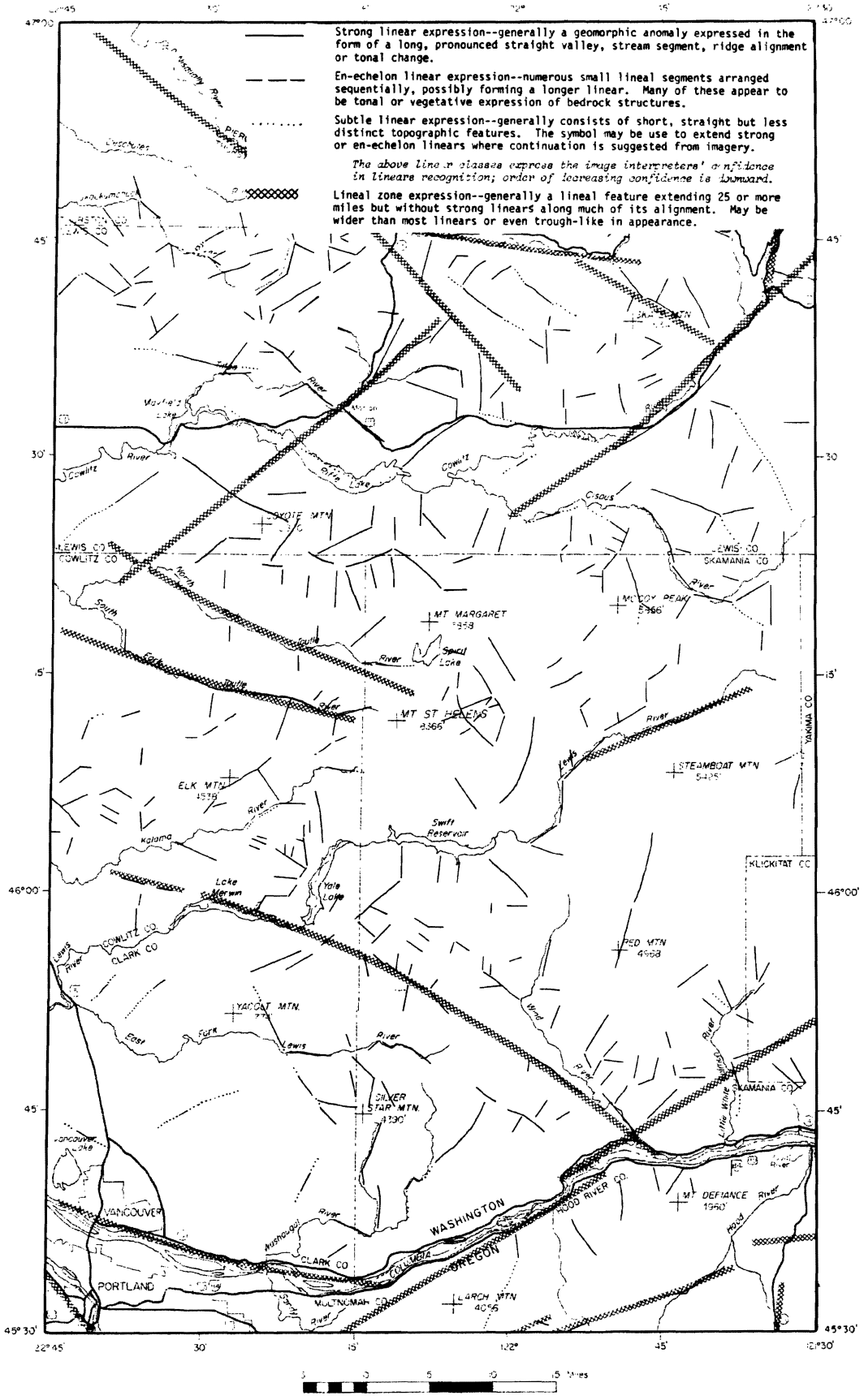

Figure 2c. Geologic lineaments of the Mount St. Helens area derived from LANDSAT MSS Band 7 images.

easy detection with East-West SLAR flight strips. Thus, absence of northerly lineaments is conservatively interpreted in Section 3.0.

The lineament analyses (Barrash and others, 1981) are based upon available satellite, U-2, and side looking airborne radar imagery and depict rationally identified topographic linear features of probable geologic origin. As such the lineaments are an indirect indication of geologic structure including faults. The lineaments, however, are not to be construed as a direct measure of faulting and therefore are put to valid use only when serving as a guide for general structural conclusions or guides to future geologic work. The lineaments have not been checked in the field.

The arrays of lineaments strongly suggest rectilinear faulting along N. 40^{o}-60^{o} W. and N. 30^{o}-50^{o} E. trends in general conformance with similar trends identified in other parts of the Cascades. The northwesterly trending lineaments trend more westerly than the postulated N. 20^{o} W. orientation of the Mount St. Helens Seismic Zone. This suggests that the zone may consist of a north northwest trending zone of northwesterly trending en echelon faults. Alternatively, the cursory lineament study is not sufficient to refute the concept of a single fault along the trend.

Regional geologic considerations outlined in the previous section suggest that a long north northwest trending fault in this area, if it does exist, probably will lie in an area of complex deformation arising from oblique subduction. It follows that a conservative mode of analysis must consider the possibility of a long single fault given the ambiguous results of the lineament analysis.

In conclusion, the St. Helens Zeismic Zone is a zone of shallow seismic activity of right lateral type for which geologic faults are not presently mapped, but for which strike slip faulting can be rationalized in terms of plate tectonic theory and available lineament data. The zone, therefore, may include: (1) a regional single fault at depth, (2) several lesser colinear, parallel, or en echelon faults in a zone or (3) volumes of rock undergoing diffuse inelastic strain in addition to more local faulting. Although evidence for a single regional fault is not compelling, such a model is adopted here because it is not conclusively eliminated by existing data and is the most conservative interpretation.

2.4 Tectonic Setting of Mount St. Helens Area

From recent research, as briefly summarized above and further presented in the selected references (Section 2.5), one can conclude the following regarding the general tectonic setting of the Western Cascades of Washington and the Mount St. Helens area in particular:

1) The area is not a major plate tectonic boundary between the North American Plate and the East Pacific Plate in the sense of the Queen Charlotte Fault. The volcano and the St. Helens Seismic Zone lie clearly within the North American Plate.
2) Because it lies clearly within the North American Plate, the region may be subject to complex intraplate deformation which may include diffuse northeast-southwest compression and northwesterly strike-slip faulting related to oblique subduction of the underlying Farallon Plate.
3) The Mount St. Helens Seismic Zone, defined by seismic activity and consistent right lateral fault plane solutions can be explained in terms of oblique subduction of an underlying plate and lies in an area of identified geologic lineaments of somewhat variable orientation. It represents one or more faults with earthquakes having focal depths of 20 km or less.
4) Although gross volcanic patterns in the Cascade Range can be broadly explained in terms of plate tectonic concepts, variations within the Range and from volcano to volcano dictate that for the purpose of rigorous siting specific vents must be evaluated on an individual basis, if possible.

2.5 Selected References

Anderson, J.L., 1980, Deformation and canyon cutting in post-Grande Ronde, pre-Frenchman Springs time, Grayback Mountain, south-central Washington: Geological Society of America Abstracts with Programs, v. 12, no. 3, p. 93.

Ando, M., and Balazs, E.I., 1979, Geodetic evidence for aseismic subduction of the Juan de Fuca plate: Journal of Geophysical Research, v. 84, no. 86, p. 3023-3028.

Armstrong, R.L., 1979, Cenozoic igneous history of the United States Cordillera from latitude 42^{o} to 49^{o} N., in Smith, R.B., and Eaton, G.P., eds., Cenozoic tectonics and regional geophysics of the western Cordillera: Geological Society of America Memoir 152, p. 265-282.

Barrash, W., Bond, J., Kauffman, J., and Shiveler, D., 1981, Geologic linears of the Cascade Range near the Oregon-Washington border: Geosciences Research Consultants unpublished report, prepared for Oregon Department of Geology and Mineral Industries, 26 p.

Bentley, R.D., 1980, Magnitude of Neogene horizontal shortening in the western Columbia Plateau, Washington-Oregon: American Geophysical Union Transactions, v. 62, no. 6, p. 60.

Carlson, R.L., 1976, Cenozoic plate convergence in the vicinity of the Pacific Northwest: A synthesis and assessment of plate tectonics in the northeastern Pacific: Seattle, Wash., University of Washington doctoral dissertation, 129 p.

Christiansen, R.L., and McKee, E.H., 1979, Late Cenozoic volcanic and tectonic evolution of the Great Basin and Columbia Intermontane regions, in Smith, R.B., and Eaton, G.P., eds., Cenozoic tectonics and regional geophysics of the western Cordillera: Geological Society of America Memoir, p. 283-322.

Coney, P.J., 1978, Mesozoic-Cenozoic Cordilleran plate tectonics: Geological Society of America Memoir 152, p. 33-50.

Crosson, R., 1980, Seismicity and tectonics of the Puget Sound region: Results from the Regional Seismograph Network: Seismological Society of America annual meeting, Seattle, Washington, Earthquake Notes, v. 50, no. 4, p. 58-59.

---1972, Small earthquakes, structure and tectonics of the Puget Sound region, Seismological Society of America Bulletin, v. 62, no. 5, p. 1133-1171.

Danes, Z.F., Bonno, M., Brau, E., Gilhan, W.D., Hoffman, F.F., Johansen, D., Jones, H.H., Malfait, B., Masten, J., and Teague, G.G., 1965, Geophysical investigation of the southern Puget Sound area, Washington: Journal of Geophysical Research, v. 70, p. 5573-5580.

Davis, G.A., 1977, Tectonic evolution of the Pacific Northwest: pre-Cambrian to present: PSAR WNP-¼, Amendment 23, Subappendix 2RC, p. 12RC-Rc-46.

---1981, Appendix 2.5N, Late Cenozoic tectonics of the Pacific Northwest with special reference to the Columbia Plateau: Draft-Preliminary, in Weston Geophysical Corporation, 1981, Amendment to WNP 2 FSAR WPPSS.

Eaton, G.P., 1979, Plate-tectonic model for late Cenozoic crustal spreading in the western United States, in Riecker, R.E., ed., Rio Grande Rift tectonics and magmatism: American Geophysical Union, Washington, D.C., p. 7-32.

Goff, F.E., and Myers, C.W., 1978, Structural evolution of East Umtanum and Yakima Ridges, south-central Washington: Geological Society of America Abstracts with Programs, v. 10, no. 7, p. 408.

Hill, D.P., 1972, Crustal and upper mantle structure of the Columbia Plateau from long range seismic-refraction measurements: Geological Society of America Bulletin, v. 83, p. 1639-1648.

---1980, Seismic evidence for the structure and Cenozoic tectonics of the Pacific Coast states, in Smith, R.B., and Eaton, G.P., eds., Cenozoic tectonics and regional geophysics of the western Cordillera: Geological Society of America Memoir 152, p. 145-174.

Hughes, J.M., Stoiber, R.E., and Carr, M.J., 1980, Segmentation of the Cascade volcanic chain: Geology, v. 8, p. 15-17.

Isacks, B., and Molnar, P., 1971, Distribution of stresses in the descending lithosphere from a global survey of focal mechanism solution of mantle earthquakes: Reviews of Geophysics, v. 9, p. 103-174.

Kienle, C.F., Jr., and Newcomb, R.C., 1974, Age of Cascadian tectonic structures north central Oregon and south central Washington: Proceedings of the Oregon Academy of Science, v. 10, p. 69.

Laubscher, H.P., 1981, Appendix 2.5-O, Models of the development of Yakima deformation: Draft, Preliminary, in Weston Geophysical Corporation, 1981, Amendment to WNP 2 FSAR WPPSS.

Langston, C.A., and Blum, D.E., 1977, The April 29, 1965 Puget Sound earthquake and the crustal and upper mantle structure of western Washington: Seismological Society of America Bulletin, v. 67, no. 3, p. 693-711.

Magill, J., and Cox, A., 1981, Post-Oligocene tectonic rotation of the Oregon Western Cascade Range and the Klamath Mountains: Geology, v. 9, no. 3, p. 127-131.

Newcomb, R.C., 1970, Tectonic structure of the main part of the basalt of the Columbia River Group, Washington, Oregon and Idaho: U.S. Geological Survey Miscellaneous Geological Investigations, Map I-587.

Reidel, S.P., and others, 1980, Rate of deformation in the Pasco Basin during the Miocene as determined by distribution of Columbia River basalt flows: Rockwell International, Rockwell Hanford Operations, report prepared by U.S. Department of Energy, PHO-BWI-SA-29, 43 p.

Riddihough, R.P., and Hyndman, R.D., 1977, The recent interaction between continent and ocean floor in the Pacific Northwest: Geological Society of America Abstracts with Programs, v. 9, no. 7, p. 1141, 90th Annual Meeting, November 1977, Seattle, Wash.

Robyn, T.L., 1977, Geology and petrology of the Strawberry Volcanics, northeast Oregon: Eugene, Oregon, University of Oregon doctoral dissertation, 197 p.

Scholl, D.W., 1974, Sedimentary sequences in the North Pacific trenches: in Burk, C.A., and Drake, C.L., eds., Geology of continental margins: Springer-Verlog, New York, Inc., p. 493-504.

Shannon and Wilson, Inc., 1973, Geologic studies of Columbia River Basalt structures and age of deformation, The Dalles-Umatilla region, Washington and Oregon: Boardman Nuclear Project, report to General Electric Company, 52 p.

Silver, E.A., 1971, Small plate tectonics in the northeastern Pacific: Geological Society of America Bulletin, v. 82, p. 3491-3496, 5 figs.

---1978, Geophysical studies and tectonic development of the continental margin off the western United States, latitude 34^{o} to 48^{o} N: Geological Society of America Memoir 152, p. 251-262.

Smith, R.B., 1977, Intraplate tectonics of the western North American plate: Tectonophysics, v. 37, p. 323-336.

---1979, Seismicity, crustal structure, and intraplate tectonics of the interior of the western Cordillera, in Smith, R.B., and Eaton, G.P., eds., Cenozoic tectonics and regional geophysics of the western Cordillera, Geological Society of America Memoir 152, p. 111-144.

Souther, J.G., 1977, Late Cenozoic volcanism and tectonics of the west central Cordillera of North America: Geological Society of America Abstracts with Programs, v. 9, no. 7, p. 1185, 90th Annual Meeting, November 1977, Seattle.

Taylor, R.W., and Frizell, V.A., 1979, Tertiary movement along the southern segment of the Straight Creek fault and its relation to the Olympia Wallowa lineament in the central Cascades, Washington: Geological Society of America Abstracts with Programs, v. 11, no. 3, p. 131.

Taubeneck, W.H., 1966, An evaluation of tectonic rotation in the Pacific Northwest: Journal of Geophysical Research, v. 71, no. 8, p. 2113-2120.

Tillson, D.D., 1970, Analysis of crustal changes in the Columbia Plateau area from contemporary triangulation and leveling measurements: Battelle Northwest, Document Identification No. ENWL-CC-2174.

Uyeda, S., and Kanamori, H., 1979, Back arc opening and the mode of subduction: Journal of Geophysical Research, v. 84, p. 1049-1081.

Walcott, R.I., 1978, Geodetic strains and large earthquakes in the axial tectonic belt of North Island, New Zealand: Journal of Geophysical Research, v. 83, p. 4419-4429.

Wang, Chi-yuen, 1980, Sediment subduction and frictional sliding in a subduction zone: Geology, v. 8, p. 530-533.

Weaver, C.S., Grant, W.C., Malone, S.D., and Endo, E.T., 1981, Post May 18 seismicity at Mount St. Helens: Volcanic and tectonic implications: unpublished report, 20 p, 8 figs.

Weston Geophysical Corporation, 1981, Section 2.5.1, Amendment to WNP 2 FSAR, v. 1, Draft text.

Wilcox, R.E., Harding, T.P., and Seely, D.R., 1973, Basic wrench tectonics: American Association of Petroleum Geologists Bulletin, v. 57, no. 1, p. 74-96.

Woodward-Clyde Consultants, 1980b, Seismological review of the July 16, 1936 Milton-Freewater earthquake source region: Prepared for Washington Public Power Supply System, 44 p.

Wright, L.A., and Troxel, B.W., 1973, Shallow-fault interpretation of Basin and Range structure, southwestern Great Basin, in DeJong, K.A., and Scholter, R., eds., Gravity and tectonics, New York, N.Y., John Wiley & Sons, p. 397-408.

Zoback, M.L., and Thompson, G.A., 1978, Basin and Range rifting in northern Nevada: Clues from a mid-Miocene rift and its subsequent offsets: Geology, v. 6, no. 2, p. 111-116.

3.0 SEISMIC EVALUATION OF MOUNT ST. HELENS SEISMIC ZONE RELATIVE TO TROJAN SITE

3.1 Fault Interpretation

3.1.1 General

The maximum possible earthquake for a given fault can be estimated using length of maximum possible surface rupture or by a determination of seismic moment, which then is correlated with magnitude. In addition, development of a recurrence frequency curve for the structure allows a determination of how often the maximum possible quake may occur or a judgment of whether or not such a quake will occur.

As described in Section 2.3, the Mount St. Helens Seismic Zone is a north 20^{o} west trending band of seismic activity extending a maximum distance of 100 km from Swift Reservoir on the south past Mount St. Helens to the vicinity of Alder Lake on the Nisqually River to the north.

In the following analysis, maximum possible surface rupture is analyzed using six available equations. Seismic moment is determined using the best available data for pressure drop and surface area of rupture. In a conservative approach, it is assumed that the Mount St. Helens Seismic Zone represents a single contiguous fault, although it is more probable that it represents several faults of lesser size and earthquake potential.

3.1.2 Measures of Earthquake Magnitude

Earthquake magnitude is a measure of earthquake energy based on records (seismograms) recorded on seismometers. Magnitude values are indicated with decimal numbers on a logarithmic scale and are derived from various measures of amplitudes of earthquake waves recorded on the seismogram, during an earthquake event. Thus, while a particular earthquake event has only one value for the total amount of energy released, the earthquake waves generated travel at different rates and are thus recorded at different times on seismograms. The

seismogram, then, is a record over time of all the earthquake waves generated during a particular event. The Richter magnitude familiar to earthquake reports was precisely defined by Richter as "the logarithm (to base 10) of the maximum seismic wave amplitude (in thousandths of a millimeter) recorded on a special seismograph called the Wood-Anderson, at a distance of 100 km from the earthquake epicenter." Other common measures of magnitude in present use merely reflect measurements derived from different parts of "wave train."

The most common measures of earthquake magnitude include M_s (surface waves), M_b (body waves), and M_ℓ (local body waves). In recent years a fourth measure of magnitude, Coda magnitude (Mc), has been adopted in the Puget Sound area by Crosson (1972, 1974). With this system, magnitude is derived from the duration of the earthquake seismogram between defined limits. The magnitude (Mc) that is so defined is analogous to Richter magnitude (M) of traditional usage.

Standard relationships have been developed to allow the conversion of earthquake magnitudes (Table 1). Ambiguities that appear in the literature (Gutenberg and Richter, 1954; Richter, 1958; and Duda, 1975) in the pursuit of a unified measure of Magnitude M are reviewed by Geller and Kanamori (1977). They show (Table 1 - equations 3 and 4) that M is most closely related to M_b. It can be shown using equation 1 that for quakes greater than M_b, $M_s = 6.5$, M_s is greater than M_b. For conservative analyses of large quakes, therefore, use of M_s is desirable.

For quakes larger than $M_s \simeq 8.3 \pm 0.3$ additional energy release by the quake occurs in wave lengths too great to be measured by equipment in common usage. For these the M_s scale is said to be saturated. Here the concept of seismic moment (M_o) discussed further below (Section 3.1.3) is particularly helpful (for $M_s \simeq 8.3 \pm 0.3$ $M_o \geq 10^{28}$ dyne - cm). Kanamori and Anderson (1975) relate M_o to M_s for values of M_s up to 8.0-8.5. It is important to note that for values of $M_o \geq 10^{28}$ there are no corresponding values for M_s except by extrapolation. Therefore, correlating acceleration to M_s for these large quakes is not possible from an empiric standpoint.

Table 1

Relationships of various measures of earthquake magnitude

1) $M_b = 2.5 + (0.63)\ M_s$ (Gutenberg and Richter, 1956)

(Derived from amplitude/period ratio of body waves of shallow and deep focus earthquakes. M_s is determined from the amplitude of surface waves of shallow earthquakes.)

2) $M_b = 1.7 + 0.8\ M_\ell - 0.1\ M_\ell^2$ (Gutenberg and Richter, 1956)

(M_ℓ is derived from the amplitude of body waves of local earthquakes.)

3) $M = 1/4\ M_s + 3/4\ (1.59\ M_b - 3.97)$ (Geller and Kanamori, 1977)

(For great shallow earthquakes)

4) $M = 1.59\ M_b - 3.97$ (Geller, 1977)

(For quakes at depths of 40-60 km)

5) $M_c = -2.46 + 2.82\ \text{Log}\ (F-P)$ (Crosson, 1974)

(M_c is derived from duration between P [arrival of P wave] and F [time after which the signal consists only of background for 10 or more seconds].)

6) $M = 2/3\ \text{Log}\ M_o - 10.7$ (Hanks and Kanamori, 1979)

(M_o is seismic moment in dyne-centimeters.)

3.1.3 Earthquake Magnitude as a Function of Source Parameters

Empirical relationships between surface rupture on faults and earthquake magnitudes have been developed (Table 2). The mathematical descriptions are broadly consistent but differ slightly owing to sampling population. Also, surface rupture (the parameter measured) is only indirectly related to other elements of the earthquake which have a bearing on earthquake magnitudes, such as energy released, our measurement of the energy released, stress drop, relative locations of observing stations, energy distribution within the total seismic spectrum, and actual vertical and horizontal dimensions of the fault rupture in the subsurface.

A comparison of observed surface rupture lengths along faults in California and Nevada (Tocher, 1958) with actual mapped lengths of the earthquake-producing faults suggests that generally 50 percent or less of a fault ruptures at the surface during moderate to large earthquakes. It is unlikely that a strike-slip fault would be active along its total geologic length in any one earthquake episode. Likewise, specific knowledge of a given fault may allow assignment of a different value to the percent active in any given event. Traditional values of 0.50 have been adopted for strike-slip faults in reactor siting in Oregon. The Washington Public Power Supply System adopted a value of 0.25 for Nuclear Project No. 1 (WPPSS, n.d.).

For the Mount St. Helens seismic shear zone the most conservative approach is to assume that the total zone represents a single fault (100 km) and that the fault is active along 50 percent of its length (50 km) in a maximum possible quake event. Available rupture-length equations (Table 2) yield a maximum possible quake of 6.0-7.4. Assuming the zone represents more than one fault, or activity along 25 percent (25 km) of the total length of a single fault (100 km), a maximum possible quake of M 5.7 to 7.1 (Table 2) is indicated.

Table 2

Determination of maximum possible earthquake
assuming surface rupture length of 50 km and 25 km

Equation	Earthquake (50 km)	Magnitude (25 km)
$M = 1.130 \text{ Log } L_{km} + 5.185$ (Housner, 1970)	7.1	6.8
$M = 1.9 \text{ Log } L_{cm} - 6.7$ (Wyss and Brune, 1968)	6.0	5.7
$M = 0.98 \text{ Log } L_{cm} + 0.75$ (Tocher, 1958)	7.3	7.0
$M = 0.76 \text{ Log } L_{cm} + 2.27$ (Iida, 1965)	7.4	7.1
$M = 1.06 \text{ Log } L_{cm} + 0.23$ (Press, 1967	7.3	7.0
$M = 1.6 \text{ Log } L_{cm} - 3.5$ (Press, 1967)	7.2	6.9

L = length of surface rupture

3.1.4 Earthquake Magnitude Determined by Seismic Moment

Earthquake magnitude based on seismograph records is really only a measure of the flux of energy or amplitude of seismic waves measured at a site within a narrow frequency band (20 seconds for M_s; 1 second for M_b). Thus, magnitude is somewhat arbitrary in terms of total energy occurring in the total seismic spectrum, and, therefore, total energy released by the earthquake. As noted above (3.1.2) this limitation is particularly significant with the larger historic earthquakes worldwide for which proportionally greater amounts of total energy released occur in the longer wave lengths not detected by conventional recording instruments.

The concept of seismic moment (Table 3) allows the development of quantitative relationships between energy released, surface area of fault activity, stress drop, rigidity, average displacements, and slip rate. Further, it has been shown that seismic moment can be related to the more traditional types of measurement of earthquake magnitude (Kanamori and Anderson, 1975). Thus, seismic moment allows more sophisticated treatment of source parameter data with magnitude. It also allows us to link these data with geologic concepts. For example, slip rates can be derived mathematically or by field measurement (Wyss and Brune, 1968; Hanks, 1975). Other geologic observations or assumptions such as active fault dimensions, rigidity, displacement, or stress drop can be translated into seismic moment.

Given the area of rupture (inferred from determination of the aftershock area) and the stress drop (inferred from knowledge of geology or determined from seismic records) it is possible to derive seismic moment (energy release). Seismic moment, in turn, has been correlated with magnitude (M_s, Kanamori and Anderson, 1975; M, Table 1, Equation 6) of more traditional usage.

It is possible to correlate area of rupture and stress drop with magnitude directly (Kanamori and Anderson, 1975). Boore (1977) demonstrates for a large population of quakes the vailidty of these relationships (Figure 4).

Seismic moment (M_0) and Richter magnitude (M) for the maximum possible quake in the Mount St. Helens Seismic Zone can be estimated using equations 7 and 8 (Table 3) if surface area of rupture and pressure drop are known. Table 4 is a matrix of values leading to estimates of M using equation 8. It is assumed

that the rupture measures 50 km by 20 km or 25 km by 10 km. For each of the two assumptions of area, pressure drops of 50 and 100 bars are assumed. The resulting range of four values for M vary from 6.6 to 7.4.

Data are not sufficient to rule out the possibility of a single fault extending the full length of the Mount St. Helens Seismic Zone. Thus, a conservative estimate of the length of rupture (50% of fault length) yields a rupture length of 50 km. Historic seismicity indicates a depth of 20 km. Thus, a rupture area of 1000 km^2 is selected.

Stress drops for earthquakes worldwide generally are between 10 and 100 bars (10^7 to 10^8 dynes/cm^2). For intraplate locations, values of 100 bars are possible, although values of 10 bars have been interpreted for some areas of strike slip faulting (Wyss and Brune, 1968). For the seismic zone in question a value of 50 bars seems reasonable. As shown on Table 5, a pressure drop of 50 bars can be estimated for the Elk Lake earthquake of February 13, 1981. Thus, using seismic moment (M_0), a Richter magnitude (M) value of 7.2 is derived from Table 4 for the maximum possible earthquake.

Table 3. Seismic moment

7) $M_o = \mu S \bar{D}$ where:

M_o = Seismic moment expressed in dyne-cm.

μ = Rigidity expressed in dynes/cm^2: Kanamori and Anderson (1975) adopt a general value of 3×10^{11} dynes/cm^2. Wyss and Brune (1968) adopt a similar value, but also adopt a value of 1.5×10^{11} dynes/cm^2 for shallow earthquakes in part of California.

S = Fault area in cm^2: Equivalent in size to area of aftershocks on the fault plane.

$\bar{D}$ = Average displacement in cm.

8) $\text{Log } M_o = \frac{3}{2} \text{ Log } S + \text{Log } \left[16\Delta\sigma/7\pi^{\frac{3}{2}}\right]$ $\left[M_o = (16/7)\,\Delta\sigma\,(S/\pi^{\frac{3}{2}}\right]$ where:

$\Delta\sigma$ = Stress drop in dynes/cm^2: Kanamori and Anderson (1975) show that stress drop is proportional to the product of rigidity (μ) and average displacement ($\bar{D}$).

Stress drop for the quoted studies is 30 bars* for plate boundaries and 100 bars for intraplate settings yielding an accepted average of 60 bars overall (Kanamori and Anderson, 1975).

Wyss and Brune (1968) show a value of less than 10 bars for a segment of the San Andreas Fault in California involving small earthquakes.

* one bar = 10^6 dynes/cm^2.

9) $M = \frac{2}{3} \text{ Log } M_o - 10.7$ (Hanks and Kanamori, 1979)

M_o = Seismic moment

M = Richter magnitude

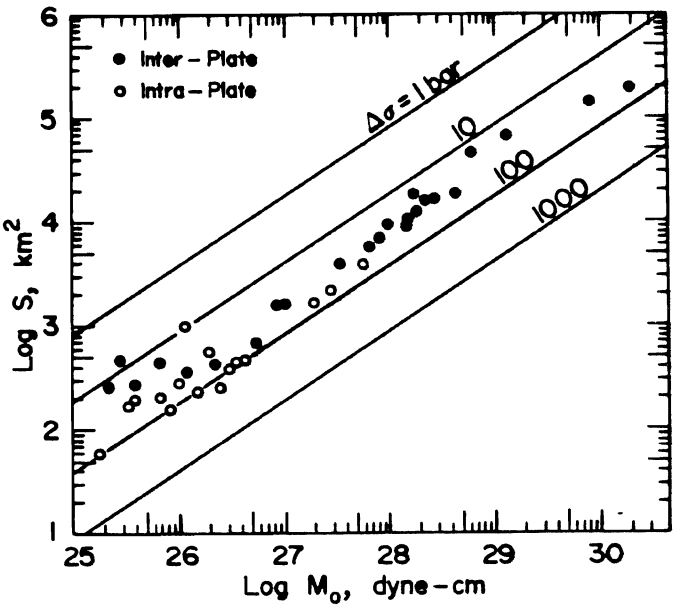

Figure 3. Relation between S (fault surface area) and Mo (seismic moment) (after Kanamori and Anderson, 1975).

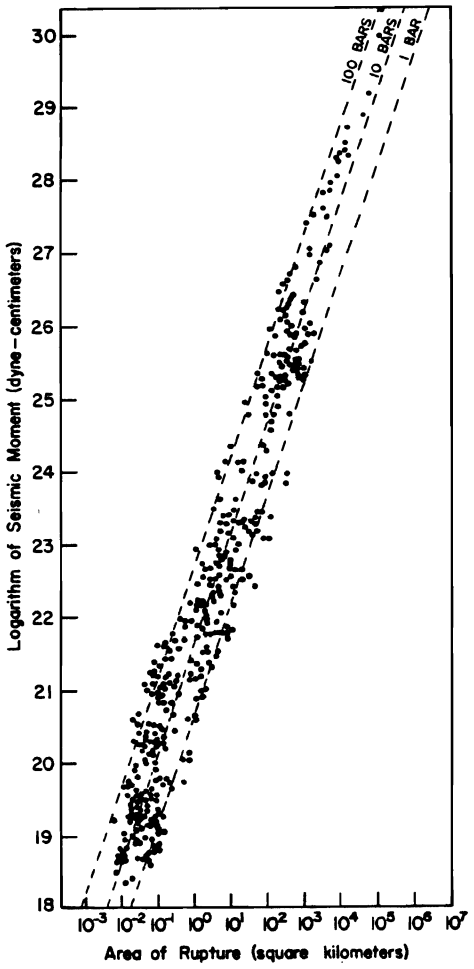

Figure 4. Relation of area of rupture to log Mo for large population of earthquakes (from Boore, 1977): Stress drop is independent of size of earthquake. Scatter for smaller earthquakes may be due to experimental error.

Table 4

Calculation of Richter magnitude of maximum possible earthquake using seismic moment and given surface area of rupture and pressure drop

Area	3/2 Log S[1]	Log $\left[16\ \Delta\sigma/7\pi^{3/2}\right]$[2]		Log M_o	M[3]
1000 km^2	19.5	7.31	(50 bars)	26.8	7.2
	19.5	7.61	(100 bars)	27.1	7.4
250 km^2	18.6	7.31	(50 bars)	25.9	6.6
	18.6	7.61	(100 bars)	26.2	6.8

1/ S is area in cm^2.

2/ $\Delta\sigma$ is pressure drop in dynes/cm^2;
Log $\left[16\ \Delta\sigma/7\pi^{3/2}\right]$ = 5.61 + Log_{10} bars. This conversion consolidates the constants including 1 bar = 10^6 dynes/cm^2.

3/ M = 2/3 Log M_o -10.7.

Table 5

Estimation of pressure drop for Elk Lake earthquake of February 13, 1981

$M = 5.5$ (oral communication, Steve Malone, 1981)

$S = 20\ km^2 \pm$ (oral communication, Craig Weaver, 1981)
$= 2 \times 10^{11}\ cm^2$

$M = 2/3 \log M_o - 10.7 = 5.5$ (Equation 9, Table 3)
Thus, $\log M_o = 24.3$

$24.3 = 3/2 \log S + \log 16\Delta\sigma/7\pi^{3/2}$ (Equation 8, Table 3)

$24.3 = 3/2\ (11.3) + 5.61 + \log_{10}$ bars (Footnote 2, Table 4)

$1.7 = \log_{10}$ bars

Bars = 50

Note:-If final estimates of S are greater than 20 km, then estimated pressure drop will be less than 50 bars.

3.1.5 Recurrence Frequency of Maximum Possible Earthquake

Maximum earthquake recurrence frequencies are derived from the equation Log N = A-bm where N is the cumulative number of events of a given magnitude, or lesser magnitude per year, A is a constant characteristic of the region, M is the magnitude, and b is the slope defined by the data. The equation represents the general distribution through time of earthquakes for a selected region or structure.

Interpretation of recurrence frequency curves requires appreciation of the limitations of the data. Commonly small quakes seem to occur at rates less than expected owing to lack of detection. Large quakes may be inadequately represented owing to incompleteness of the historic record. Where the curve is defined primarily on the basis of earthquakes in the mid-magnitude range in this way, efforts would be made to constrain the upper and lower ends of the curve.

A recurrence frequency curve statistically defines the frequency with which earthquakes of a given magnitude can be expected statistically. Viewed alone a recurrence frequency curve does not define the maximum possible earthquake for a region, however. Accomplishment of this task requires an estimate of the period of time between the maximum possible quakes for the area. Sykes (1965), for example, provides time estimates for various parts of the world. Molnar (1979) conceptualizes a manner in which plate tectonics and seismic moment can be linked to place limits on frequency curves. This type information then can be used to infer the maximum possible quake for an area using a recurrence frequency curve.

Knowledge of the maximum possible quake derived by independent means can be used in conjunction with the recurrence frequency curve to derive the frequency with which the maximum possible earthquake will occur. This is the primary value of the recurrence frequency curve technique in this study as shown below.

Weaver and Smith (1981) plot 14 earthquakes ($2.8 < Mc < 5.5$) representing an 11-year period (1970-1980) to define the Mount St. Helens Seismic Zone (Section 2.3). Smaller quakes are not considered owing to poor resolution and the possibility of other sources such as blasting or other small structures. To construct a conservative frequency curve here, all quakes with $Mc \geq 2.0$ located

within 5 km of a N. 20° W. trending line from Mount St. Helens towards Puget Sound (to latitude 46°45') are tabulated (Table 6). The data represent the period 1971-1978 for which well instrumented data are available in published form. The data constitute a very conservative data base upon which to construct a recurrence frequency curve.

The data set is unconstrained for low magnitudes by design and it is unconstrained at high magnitudes owing to the short period of observation. A slope for a recurrence frequence curve is, therefore, not well defined by the data. Instead, the data represent a point or short segment of such a curve. Crosson (1972) determines a slope of -0.96 for a broad population of shallow historic earthquakes in the Puget Sound area. The figure of -0.96 = b is the most realistic figure for long term projections given the abnormal seismic activity bracketing the eruption of Mount St. Helens. A general recurrence frequency curve for the Mount St. Helens Seismic Zone based on the above assumption is given in Figure 5 and is represented by the equation Log N = -0.96 M + 2.78.

For the immediate Mount St. Helens area, Endo and others (1981) determine a slope b = 0.6 for pre-eruption quakes; Weaver and others (1981) determine a slope of b = 0.67 for post-eruption quakes. These figures are not appropriate for the total Mount St. Helens Seismic Zone given the short time frame of their observation and geographic restriction to the Mount St. Helens area.

Although instrumentation was poor prior to 1970, additional data (Table 7) are adequate to suggest the absence of large quakes along or near the Mount St. Helens Seismic Zone between 1893 and 1978. The recurrence frequency (Figure 5), based on data over a short time frame, is consistent with these data representing a larger (historic) time frame and appears, therefore, to be valid.

The preliminary curve also shows that a quake of magnitude (M) 7.2 will occur statistically once every 10,000 years. It is concluded that if the Mount St. Helens Seismic Zone represents a single fault (100 km) and if the fault ruptures along one-half its length (50 km) to yield a maximum possible quake, then such a quake will probably occur about once every 10,000 years. The short time span of observation is evident in Table 6 and Table 7 and may not be adequate for large extrapolations.

If it is assumed that maximum possible quakes for a region occur once every few hundred years consistent with the data of Sykes (1965), then the maximum possible quake for the Mount St. Helens Seismic Zone is clearly less, being on the order of 5.2 for a 100-year recurrence frequency or 6.2 for a 1,000-year recurrence frequency.

As a matter of geologic judgment it would seem unreasonable that stress would accumulate for a period of 10,000 years prior to release in the largest possible quake in the fault zone. It is more likely that stress will be relieved in other ways over shorter time frames. Time frames of a few hundreds of years are more realistic worldwide (Sykes, 1966). Thus, the indication from the preliminary frequency curve that the largest possible quake conservatively determined from source parameters and seismic moment (M = 7.2) is probably too large in view of the historic record.

3.1.6 Summary

If one assumes that a single earthquake producing fault extends the length of the Mount St. Helens Seismic Zone, then a maximum quake with Richter Magnitude M = 7.2 is possible. A rupture 50 km long and 20 km deep with a pressure drop of 50 bars is assumed. Source parameter calculations of traditional usage yield similar values to those derived through consideration of seismic moment concepts.

Considerations of lineament distributions (2.3), recorded earthquake history for the Pacific Northwest, and earthquake recurrence frequency for the Mount St. Helens Seismic Zone (Figure 5) indicate that estimates of M = 7.2 are probably too high. A maximum possible earthquake in the range 5.2 - 6.2 appears more likely. However, the possibility of a single fault extending 100 km along the Mount St. Helens Seismic Zone cannot be totally ruled out on the basis of data now available. This is particularly true given the facts that regional geologic structures are poorly identified and the recurrence frequency curve is based on rather limited data.

Table 6

Seismicity of Mount St. Helens Seismic Zone 1971-1978 (Mc ≥2.0)

Date	Magnitude (Mc)	Depth (km)	Date	Magnitude (Mc)	Depth (km)
5/28/1971	3.4	22.1	9/17/1975	2.9	6.6
6/12/1971	2.7	13.4	9/17/1975	2.0	1.7
12/29/1971	2.4	18.7	9/25/1975	2.0	7.0
			10/8/1975	2.7	8.0
2/9/1972	2.2	17.3	10/11/1975	2.6	13.3
3/31/1972	2.3	16.8	10/12/1975	2.2	12.6
4/19/1972	2.5	9.0			
6/16/1972	2.4	8.9	5/8/1976	2.1	19.5
10/7/1972	2.5	1.0F	8/19/1976	2.2	9.8
10/13/72	2.4	1.0F	10/10/1976	2.0	1.0F
10/13/1972	2.6	1.0F	10/14/1976	4.0	9.9
10/27/1972	2.1	1.0F			
11/10/1972	2.1	24.1	1/12/1977	7.6	1.0F
			2/25/1977	2.9	24.7
2/27/1973	2.7	21.0	2/25/1977	3.0	23.4
3/15/1973	2.1	10.0	5/5/1977	3.2	6.4
4/7/1973	3.0	25.2	5/22/1977	2.9	3.8
4/19/1973	3.4	0.3	5/30/1977	3.0	25.4
8/25/1973	2.7	3.0	6/7/1977	2.6	8.8
9/5/1973	2.4	6.0	6/20/1977	2.4	7.7
			6/26/1977	2.5	6.0
5/21/1974	3.5	11.2	7/14/1977	2.7	6.8
7/31/1974	2.0	9.7	8/6/1977	2.1	6.6
8/31/1974	2.0	4.7	9/17/1977	2.0	10.1
10/7/1974	2.5	1.4	9/18/1977	2.1	13.7
			11/20/1977	2.1	20.0
			1978	None	

Note: F Indicates "fixed depth" to allow determination of location.

Table 7

Historic seismicity of Mount St. Helens Seismic Zone 1893-1970
(Data from WPPSS, n.d.)

Date	Intensity	Calculated Magnitide (M_s)
8/14/1893	IV	2.0
2/25/1895	V	3.0
1/7/1960	V	3.0
10/11/1960	IV	2.0
1/3/1961	IV	2.0
1/3/1961	V	3.0
1/26/1961	V	3.0
7/28/1961	IV	2.0
9/17/1961	VI	4.0
11/3/1962	IV	2.0
11/9/1962	IV	2.0
11/30/1968	V	3.0

[1] $M_b = 1 + 2/3\ I$ (Gutenberg and Richter, 1965).

$M_s = \frac{M_b - 2.5}{0.63}$ (Equation 1, Table).

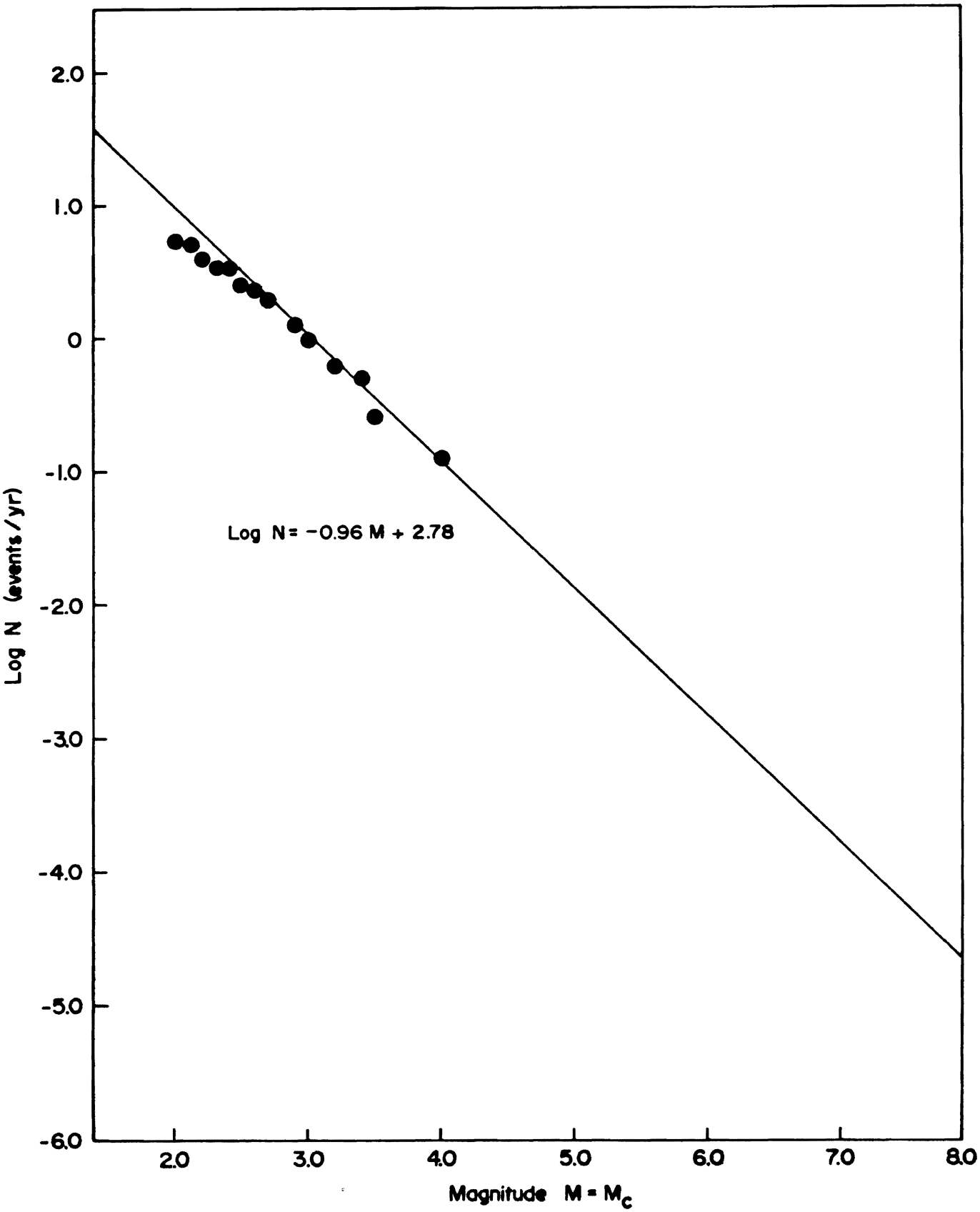

Figure 5. Generalized recurrence frequency curve for St. Helens Seismic Zone.

3.1.7 Selected References

Aki, K., 1967, Scaling law of seismic spectrum: Journal of Geophysical Research, v. 72, p. 1217-1231.

Bonilla, M.G., 1979, Historic surface faulting--map paterns, relation to subsurface faulting, and relation to pre-existing faults: Proceedings of Conference VIII, Analysis of actual fault zones on bedrock, National earthquake hazards reduction program: U.S. Geological Survey Open-File Report 79-1239, p. 36-65.

Bonilla, M.G., and Buchanan, J.M., 1970, Interim report on worldwide historic surface faulting: U.S. Geological Survey Open-file report.

Boore, D.M., 1977, The motion of the ground in earthquakes, in Earthquakes and volcanoes: Scientific American, San Francisco, W.H. Freeman and Company, p. 9-19.

Brune, J.N., 1968, Seismic moment, seismicity, and rate of slip along major fault zones: Journal of Geophysical Research, v. 73, p. 777-784.

Chinnery, M.A., 1969, Earthquake magnitude and source parameters: Seismological Society of America Bulletin, v. 59, p. 1969-1982.

Cloud, W.K., 1972, Strong motion earthquake records: Berkeley, Calif., University of California, Lecture notes, summer course.

Couch, R.W., and Lowell, R.P., 1971, Earthquakes and seismic energy release in Oregon: Oregon Department of Geology and Mineral Industries, Ore Bin, v. 22, no. 4, p. 61-84.

Crosson, R.S., 1972, Small earthquakes, structure, and tectonics of the Puget Sound region: Bulletin of the Seismological Society of America, v. 62, p. 1133-1171.

---1974, Compilation of earthquake hypocenters in western Washington: Washington Division of Geology and Earth Resources Information Circular 53, 25 p.

---1976, Crustal structure modeling of earthquake data, 2, Velocity structure of the Puget Sound region, Washington: Journal of Geophysical Research, v. 81, p. 3047-3054.

Crosson, R.S., and Frank, D., 1975, The Mt. Rainier earthquake of July 18, 1973, and its tectonic significance: Bulletin of the Seismological Society of America, v. 65, p. 549-552.

Duda, S.J., 1975, Secular seismic energy release in the circum-Pacific belt: Tectonophysics, p. 409-452.

Endo, E.T., Malone, S.D., Noson, L.L., and Weaver, C.S., (in 1981 press) Locations, magnitudes, and statistics of the March 20-May 18 earthquake sequence.

Evernden, J.F., Hibbard, R.R., and Schneider, J.F., 1973, Interpretation of seismic intensity data: Seismological Society of America Bulletin, v. 63, no. 2, p. 399-422.

Geller, R.G., 1976, Scaling relations of earthquake source parameters and magnitudes: Seismological Society of America Bulletin, v. 66, no. 5, p. 1501-1523.

Geller, R.G., and Kanamori, H., 1977, Magnitudes of great shallow earthquakes from 1907 to 1952: Seismological Society of America Bulletin, v. 67, no. 3, p. 587-598.

Gower, Howard D., 1978, Tectonic map of the Puget Sound region, Washington, showing locations of faults, principal folds, and large-scale Quaternary deformation: U.S. Geological Survey Open-File Report 78-426, 17 p., 3 figs.

Gutenberg, B., and Richter, C.F., 1954, Seismicity of the earth, 2nd edition: Princeton, New Jersey, Princeton University Press.

---1956, Earthquake magnitude, intensity, energy and acceleration: Seismological Society of America Bulletin, v. 46, p. 105-145.

Hanks, T.C., 1975, Seismic moments of larger earthquakes of the southern California region: Geological Society of America Bulletin, v. 86, p. 1131-1139, 4 figs.

Hanks, T.C., and Kanamori, H., 1979, A moment magnitude scale: Journal of Geophysical Research, v. 84, p. 2348-2350.

Hershberberger, J., 1956, A comparison of earthquake acceleration with intensity ratings: Seismological Society of America Bulletin, v. 46, no. 4, p. 317-330.

Housner, G.W., 1965, Intensity of earthquake ground shaking near the causative fault: Proceedings of the 3rd World Conference on Earthquake Engineering, New Zealand, v. 1, p. III: 94-115.

---1970, Engineering estimates of ground shaking and maximum earthquake magnitude: Proceedings of the 4th World Conference on Earthquake Engineering, Santiago de Chile, v. 1, p. 1-13.

Howell, B.F., Jr., Lundquist, G.M., and Yiu, S.K., 1970, Integrated and frequency-band magnitude, two alternative measures of the size of an earthquake: Seismological Society of America Bulletin, v. 60 (3), p. 917-937.

Iida, K., 1965, Earthquake magnitude, earthquake fault, and source dimensions: Journal of Earth Science, Nagoya University, v. 13, p. 115-132.

Isacks, B., Oliver, J., and Sykes, L.R., 1968, Seismology and the new global tectonics: Journal of Geophysical Research, v. 73, no. 18, p. 5855-5899.

Joyner, W.B., Boore, D.M., and Porcella, R.L., 1981, Peak horizontal acceleration and velocity from strong motion records, including records from the 1979 Imperial Valley, California earthquake: U.S. Geological Survey Open-File Report 81-365, 46 p.

Kanamori, H., and Anderson, D.L., 1975, Theoretical basis of some empirical relations in seismology: Seismological Society of America Bulletin, v. 65, p. 1073-1095.

Malone, S.D., Endo, E.T., and Ramey, J.W., (in 1981 press): Seismic monitoring for eruption prediction.

Molnar, P., 1979, Earthquake recurrence intervals and plate tectonics: Seismological Society of America Bulletin, v. 69, no. 1, p. 115-134.

Newmark, N.M., and Rosenblueth, E., 1971, Fundamentals of earthquake engineering: Englewood Cliffs, New Jersey, Prentice-Hall.

Page, R.A., and others, 1972, Ground motion values for use in the seismic design of the Trans-Alaska pipeline system: U.S. Geological Survey Circular 672.

Perkins, D.M., Thenhaus, P.C., Hanson, S.L., Ziony, J.I., and Algermissen, S.T., 1980, Probabilistic estimates of maximum seismic horizontal ground motion on rock in the Pacific Northwest and the adjacent outer continental shelf: U.S. Geological Survey Open-File Report 80-471, 39 p., 7 pls.

Press, F., 1967, Dimensions of the source region for small, shallow earthquakes, in Proceedings of the VESIAC Conference on the source mechanism of shallow seismic events: VESIAC Report 7885-1-X, p. 155-164.

Richter, C.F., 1958, Elementary seismology: San Francisco, Calif., Freeman and Company.

---1959, Seismic regionalization: Seismological Society of America Bulletin, v. 49, no. 1, p. 123-162.

Sauter, F.F., 1979, Damage prediction for earthquake insurance, in Proceedings of the 2nd United States National Conference on Earthquake Engineering, August 22-24, 1979: Stanford University, p. 99-108.

Seed, H.B., Idress, I.M., and Kiefer, F.W., 1969, Characteristics of rock motions during earthquakes: Journal of Soil Mechanics and Foundations Division, ASCE, v. 95, no. SM-5.

Shannon and Wilson, Inc., 1972, Seismic regionalization studies, Bonneville Power Administration service area, Washington, Oregon, Idaho and western Montana: Report to Agbabian Associates, 250 North Nash, El Segundo, Calif., 38 p.

---1975, Geotechnical investigation for central plant facilities, Pebble Springs site, Boardman nuclear project, Gilliam County, Oregon: v. 1, Summary report Appendix B - Earthquake and ground response analyses.

Sykes, L.R., 1965, The seismicity of the Arctic: Seismological Society of America Bulletin, v. 55, no. 2, p. 500-518.

Thenhaus, P.C., 1978, A study of the October 12, 1877 Oregon earthquakes: U.S. Geological Survey Open-File Report 78-234, 12 p.

Tocher, D., 1958, Earthquake energy and ground breakage: Seismological Society of America Bulletin, v. 48, p. 147-153.

Trifunac, M.D., and Brady, A.G., 1975, On the correlation of seismic intensity scales with the peaks of recorded strong ground motion: Seismological Society of America Bulletin, v. 65, no. 1, p. 139-162.

Washington Public Power Supply System, (n.d.), Preliminary safety analysis report: Washington Public Power Supply System Nuclear Project No. 1, v. 1, sec. 2.5, fig. 2.5-21.

Weaver, C.S., Grant, W.C., Malone, S.D., and Endo, E.T., 1981, Post May 18 seismicity of Mount St. Helens: volcanic and tectonic implications: Unpublished report, 20 p., 8 figs.

Weaver, C.S., Greer, S.M., and Iyer, H.M., Seismicity of Mount Hood and structure as determined from Teleseismic P. wave delay studies: Journal of Geophysical Research.

Weaver, C.S., and Smith, S.W., (in 1981, prep.), Earthquake hazard implications of crustal fault zone in western Washington: To be submitted to Bulletin of the Seismological Society of America.

Woodward-Clyde Associates, 1970, Ground motion, Trojan nuclear plant, Rainier, Oregon: Report to Bechtel Corporation, 5 p., 2 tables, 3 figs.

Wyss, M., and Brune, J.N., 1968, Seismic moment, stress, and source dimensions for earthquakes in the California-Nevada region: Journal of Geophysical Research, v. 73, p. 4681-4694.

3.2 Ground Motion at Trojan Site

3.2.1 General

The effect of a given earthquake at a given site is dependent upon the specific characteristics of the earthquake, the fault, the site, and the transmission of the seismic waves from the fault to the site. In the following analysis, acceleration, ground velocity, and displacement are determined in a conservative manner using available relationships with magnitude M, M_o = 7.2 and distance (30 miles) from the Mount St. Helens Seismic Zone to the Trojan site as determined in the previous section. For each the more conservative or realistic figure is selected where more than one figure is available. The site is bedrock. The data are then plotted on the response spectrum of the FSAR for the Safe Shutdown Earthquake for the Trojan Nuclear Power Plant. This provides a comparison with the original design considerations of the facility. Relationships are also presented for approximating earthquake duration and predominant period.

3.2.2 Acceleration

The relationship of ground acceleration at a site to earthquake magnitude and to distance from the epicenter is presented graphically by Housner (1965) (Figure 6), Cloud (1972) (Figure 7), Seed and Idriss (1970) (Figure 8), Schnabel and Seed (1973) (Figure 9), and Boore and others (1978) (Figure 10). Although the graphs are based in part on different sets of data from different areas, they display a general consistency for sites more than a few miles from an epicenter. Boore and others (1978) distinguish between rock sites and soil sites. Joyner and others (1981) develop an equation for deriving acceleration from magnitude and distance (Table 8).

Joyner and others (1981) use carefully selected data to develop an equation to determine acceleration givem moment magnitude, distance, and site geology (Table 8). The data are representative of shallow earthquakes of western North

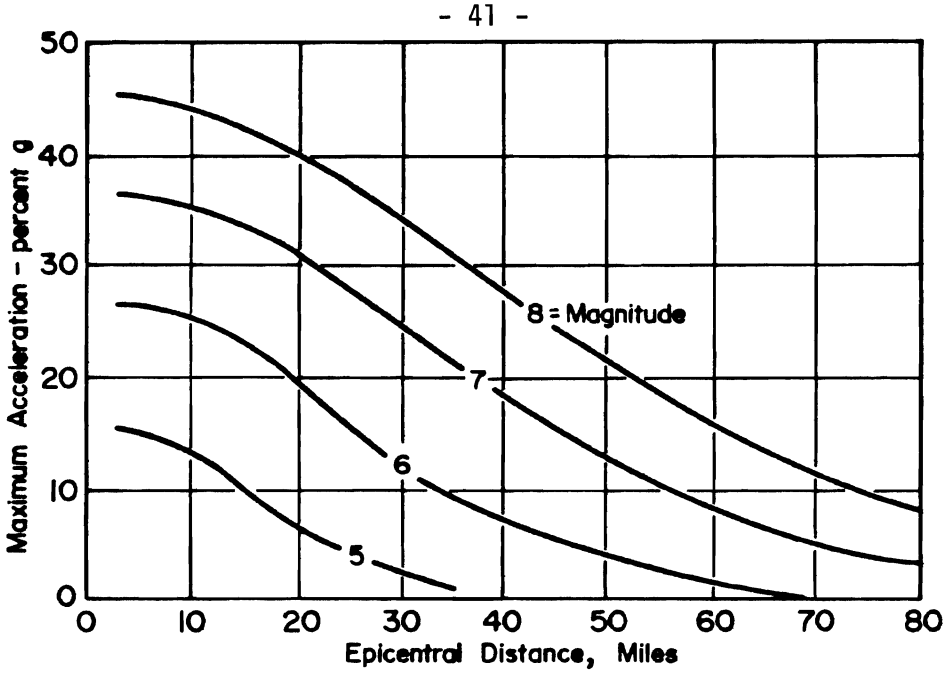

Figure 6. Relationship of maximum acceleration, epicentral distance, and magnitude for firm ground by Housner, 1965.

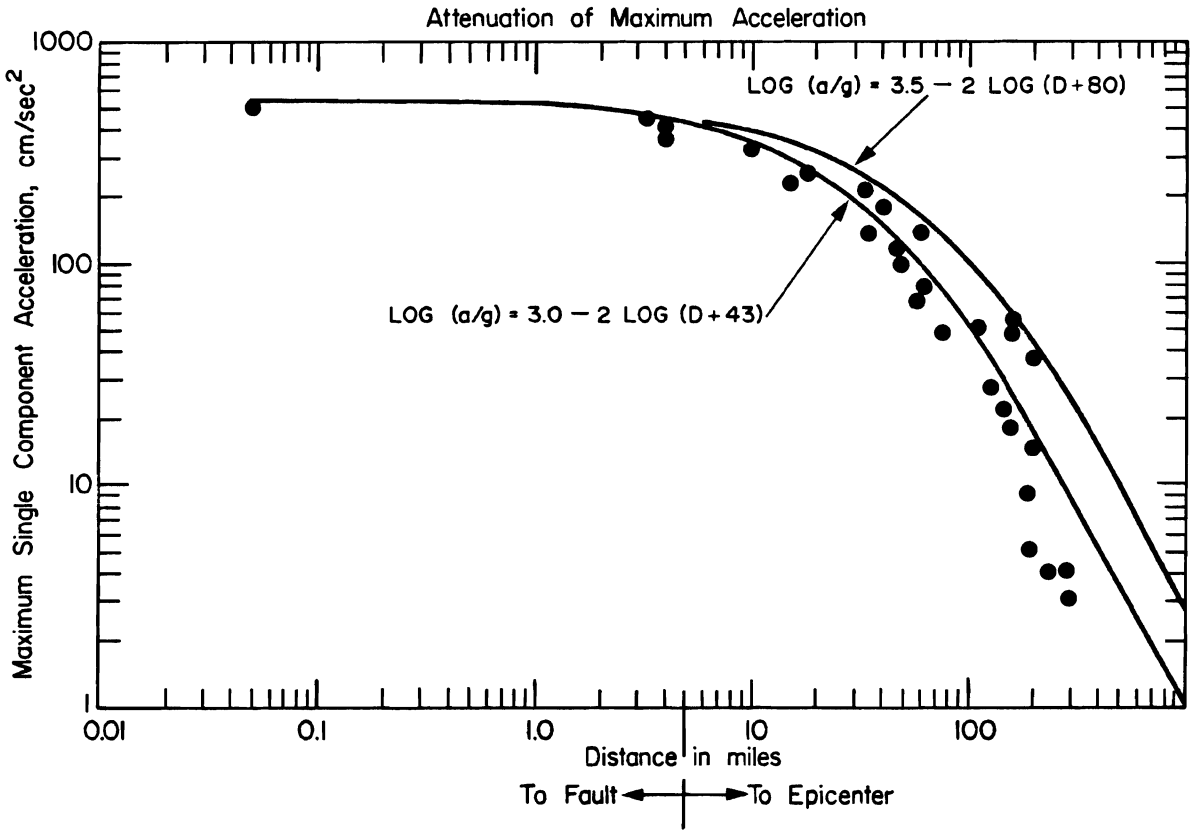

Figure 7. Relationship between peak ground acceleration and distance from fault by Cloud and Perez, 1971.

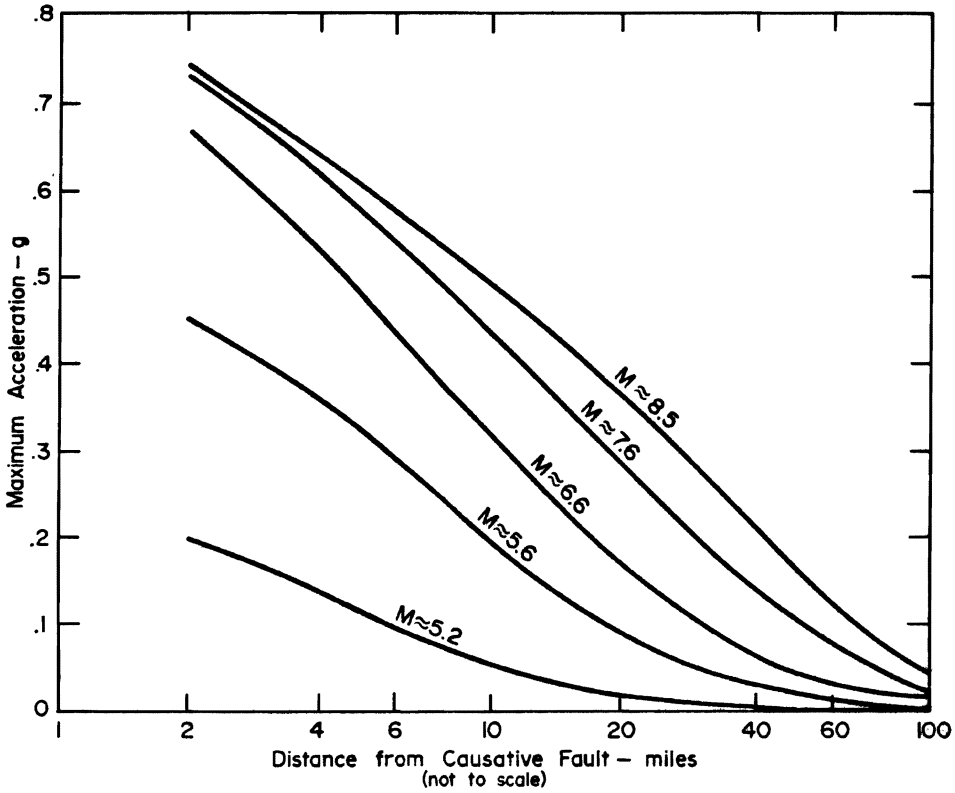

Figure 8. Relationship between maximum acceleration in rock, earthquake magnitude, and distance from causative fault from Seed and Idriss, 1970 (in Shannon and Wilson, 1974).

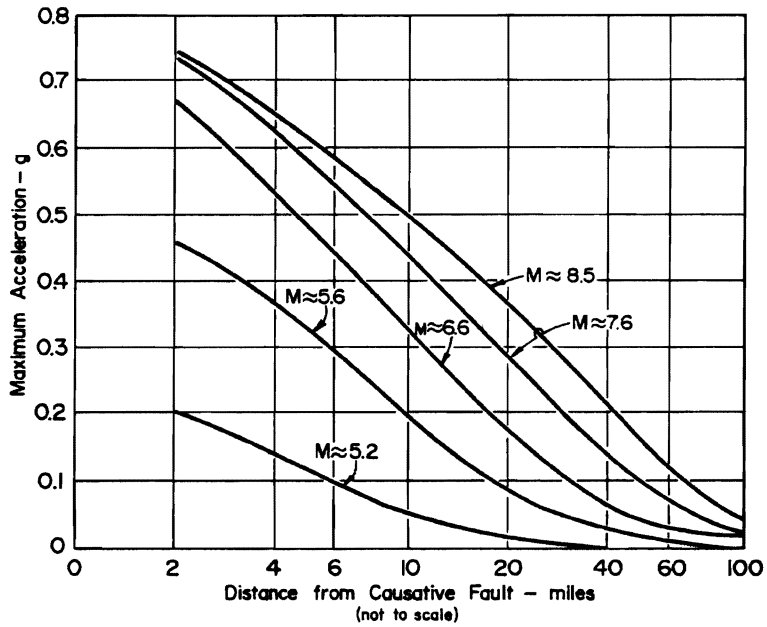

Figure 9. Relationship of maximum acceleration to epicentral distance and magnitude for rock by Schnabel and Seed, 1973 (in Shannon and Wilson, 1974).

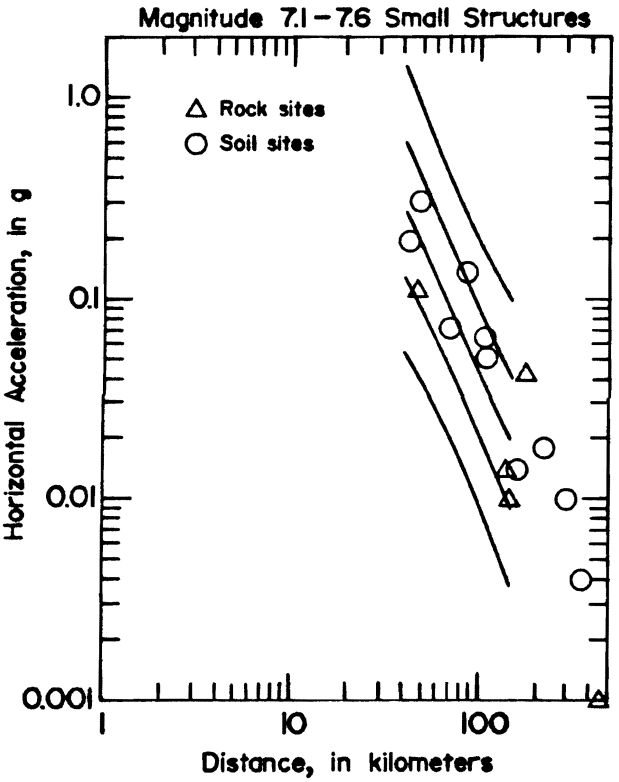

a) *Peak horizontal acceleration versus distance to slipped fault for magnitude range 7.1-7.6.*

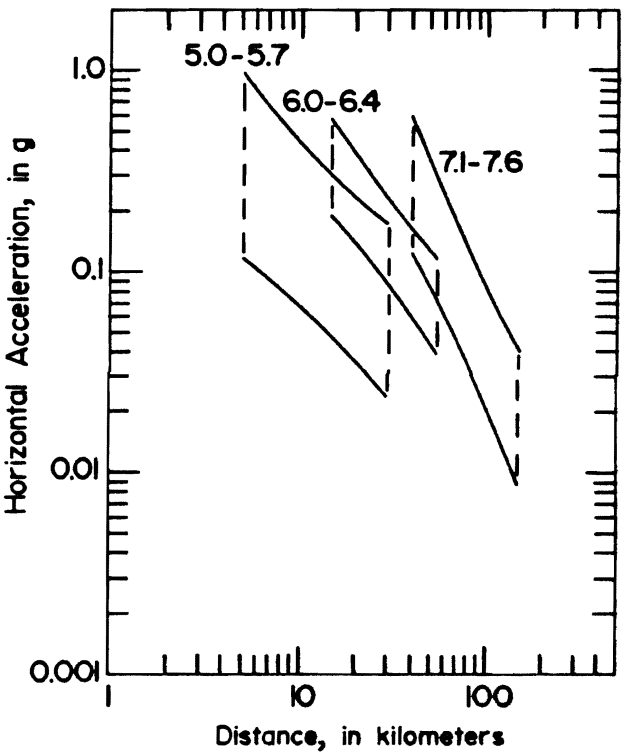

b) *Comparison of 70 percent prediction intervals for peak horizontal acceleration recorded at base of small structures for magnitude classes 5.0-5.7, 6.0-6.4, 7.1-7.6.*

Figure 10. Relationship of horizontal acceleration to distance and magnitude according to Boore and others, 1978.

America and are manipulated with improved methods of statistical analysis. The seismic zone in question falls within the range of the published data in terms of magnitude and distance.

Assuming a maximum possible earthquake of magnitude M, M_o = 7.2 at a distance of 30 miles (50 kilometers) the following values are derived for acceleration:

Housner (1965)	Figure 6	0.27 g
Cloud and Perez (1971)	Figure 7	0.25 g
Seed and Idriss (1970)	Figure 8	0.15 g
Schnabel and Seed (1973)	Figure 9	0.17 g
Boore and others (1978)	Figure 10	0.15 g
Joyner and others (1981)	Table 8	0.17 g

The more recent models are derived from more comprehensive and refined data sets. They give greater consideration of ground conditions and are based on more thorough statistical analysis. Thus, a maximum possible acceleration of 0.17 g is selected. Use of the same equation (10) for the February 13, 1981 Elk Lake earthquake (M = 5.5, d = 63 km) yields a maximum acceleration of 4 percent of g at the Trojan plant, although the distance involved is outside the data set for earthquakes of this magnitude in the study (see Figure 10b).

Table 8. Calculation of acceleration at a point 50 kilometers from an M, M_o = 7.2 earthquake using the technique of Joyner and others, 1981

10) $\log A = -1.23 + 0.280\, M_o - \log r - .00255\, r + 0.27\, P$

$\log A = -1.23 + 2.02 - 1.70 - .13 + .27$

$\log A = -.77$

$A = 17\%\ g$

A = Acceleration in percent of g

$r = (d^2 + 7.3^2)^{\frac{1}{2}}$

M_o = Moment magnitude (= 7.2)

P = 1 for rock sites

d = Distance in kilometers (= 50 km)

3.2.3 Velocity, Displacement and Predominant Period

The relationship of velocity at a site to earthquake magnitude and to distance from the epicenter is analyzed by Newmark and Hall (1969), Boore and others (1978) (Figure 11), (1980), Seed and others (1976), Mohraz (1976), and Joyner and others (1981) (Table 9). Newmark and Hall (1969) suggest a conservative approach involving a "standard earthquake" which by definition yields the characteristics shown below:

Standard Earthquake of Newmark and Hall (1969)

$a = 0.5\ g$
$v = 2.0$ feet per second
$d = 0.6$ feet

By determining g at a site one can in a very conservative manner derive v and d using simple proportions. For $g < 0.5$ this is conservative as a study of data presented by Boore and others (1978, 1980), Seed and others (1976), and Mohraz (1976) shows. For velocity and displacement, all data plots of Boore and others (1978) are for sites underlain by soil (>4-5 M) rather than rock, and therefore are probably high for comparable sites on rock such as the Trojan site.

Joyner and others (1981) use carefully selected data to develop an equation to determine velocity given earthquake moment magnitude (M_0), distance, and site geology. The data are representative of shallow earthquakes of western North America and are manipulated with improved methods of statistical analysis. The seismic zone in question in this study falls within the range of their data in terms of magnitude and distance (Table 9).

Assuming a maximum possible earthquake of magnitude 7.2 at a distance of 30 miles (50 kilometers) the following values are derived for velocity:

Newmark and Hall (1969)		17 cm/sec
Boore and others (1978)	Figure 11	22 cm/sec
Joyner and others (1981)	Table 9	25 cm/sec

The figure of 25 cm/sec is the most recent and conservative and is adopted as the maximum possible velocity.

Newmark and Hall (1969) and Boore and others (1978) (Figure 12) analyze the relationship of displacement to magnitude and distance. Assuming an earthquake of magnitude (M, M_o) = 7.2 at a distance of 30 miles (50 kilometers) a maximum possible displacement of 10 cm is indicated.

Seed and Idriss (1970) (Figure 13) present the relationship of predominant period to magnitude and distance. A predominant period of approximately 0.35 seconds is indicated.

Dobry and others (1978) and Boore and others (1978) (Figure 14) relate duration in hard rock to magnitude as follows:

$$11) \quad \text{Log } D = 0.432\ M - 1.83$$

For an earthquake of magnitude 7.2, a duration of 19 seconds is indicated.

Table 9. Calculation of velocity at a point 50 kilometers from an M, M_o = 7.2 earthquake using the technique of Joyner and others, 1981

$$12) \quad \text{Log } v = -1.30 + 0.581\ M_o - \text{Log } r - .00256\ r + 0.175\ S + .35\ P$$

$$\text{Log } v = -1.30 + 4.18 - 1.70 - 0.13 + 0 + 0.35$$

$$\text{Log } v = 1.40$$

$$v = 25 \text{ cm/sec}$$

---

v = Velocity in cm/sec

r = $(d^2 + 7.3^2)^{\frac{1}{2}}$

M_o = Moment magnitude

S = 0 for rock sites; 1 for soil sites

P = 1 for rock sites

d = Distance in kilometers

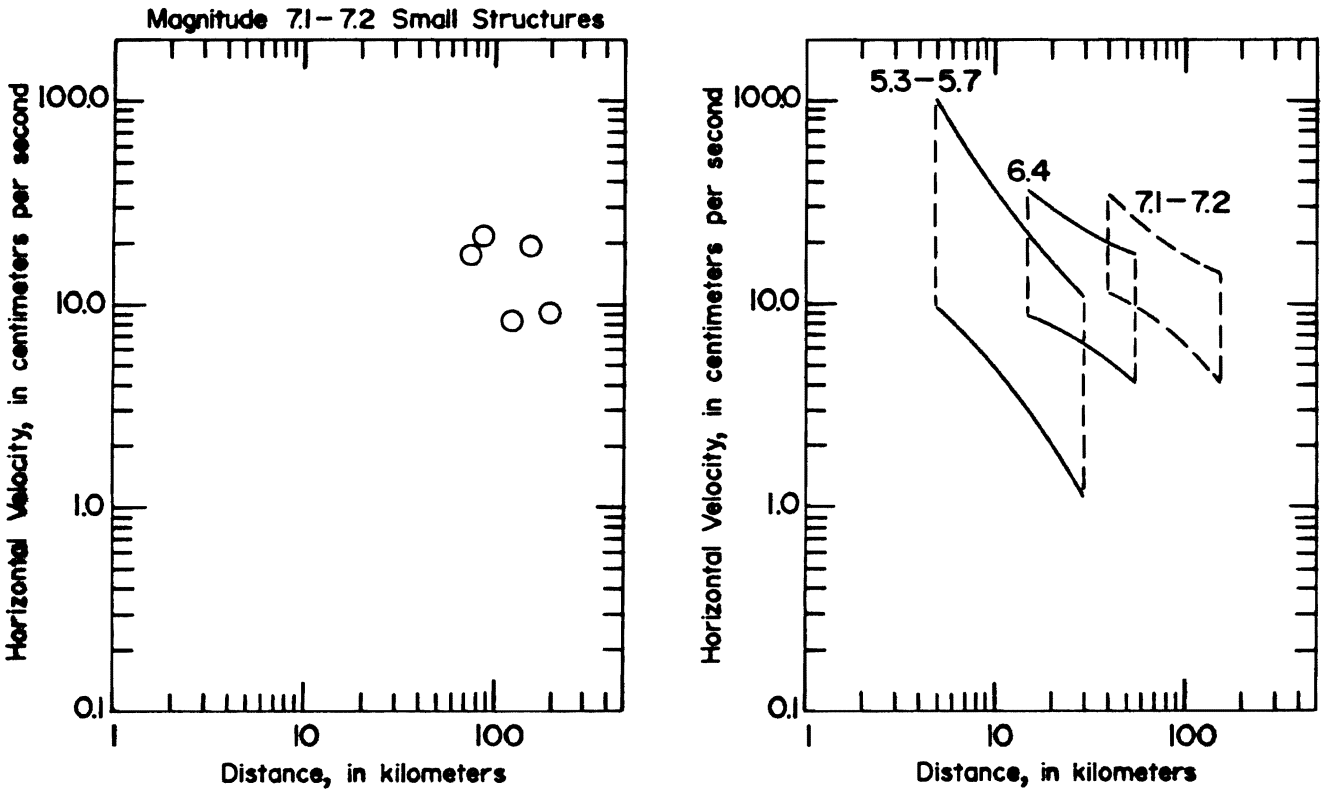

a) *Peak horizontal velocity versus distance to slipped fault for magnitude range 7.1-7.2 recorded at base of small structures (soil sites).*

b) *Comparison of 70 percent prediction intervals for peak horizontal velocity recorded at base of small structures for three magnitude classes 5.3-5.7, 6.4, and 7.1-7.2.*

Figure 11. Relationship of horizontal velocity to distance and magnitude according to Boore and others, 1978.

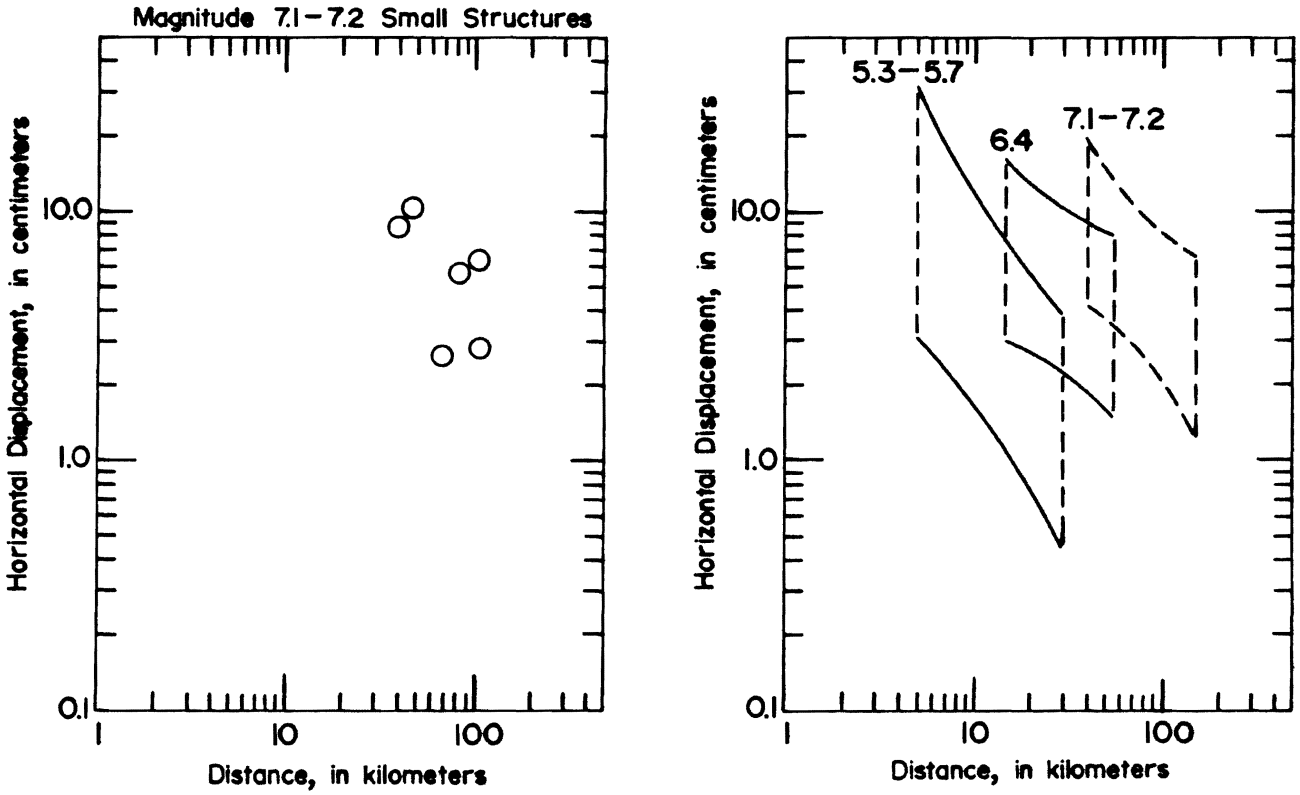

a) *Peak horizontal displacement versus distance to slipped fault for magnitude 7.1-7.2 recorded at base of small structures.*

b) *Comparison of 70 percent prediction intervals for peak horizontal displacement recorded at base of small structures for three magnitude classes 5.3-5.7, 6.4, and 7.1-7.2.*

Figure 12. Relationship of horizontal displacement to distance and magnitude according to Boore and others, 1978.

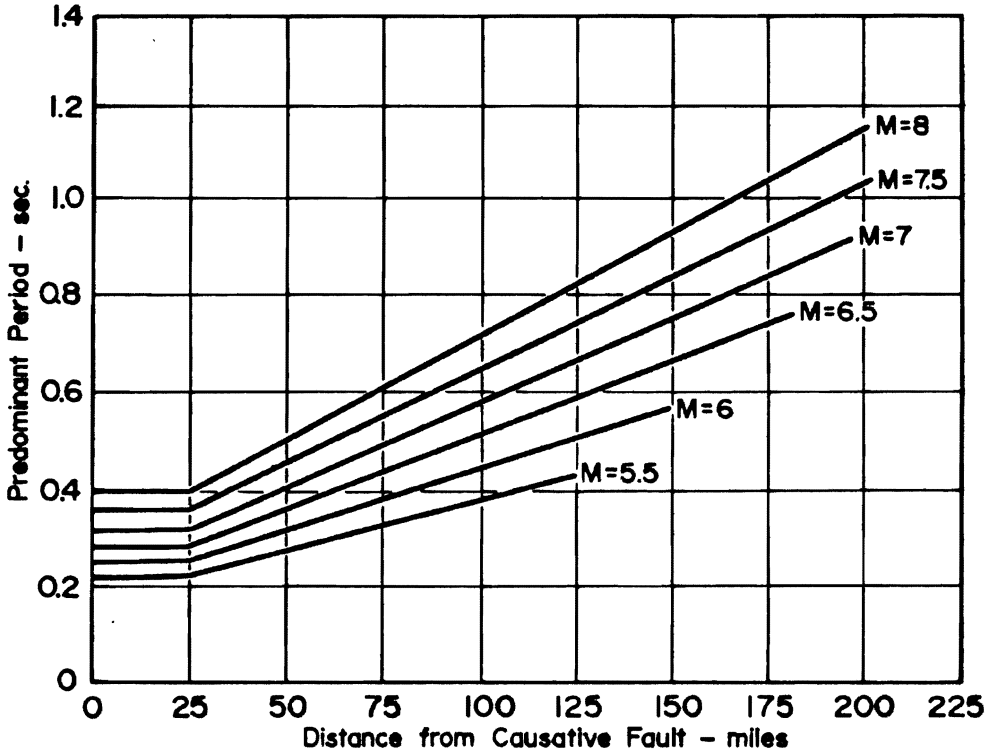

Figure 13. Predominant periods for maximum accelerations in rock by Seed and Idriss, 1970.

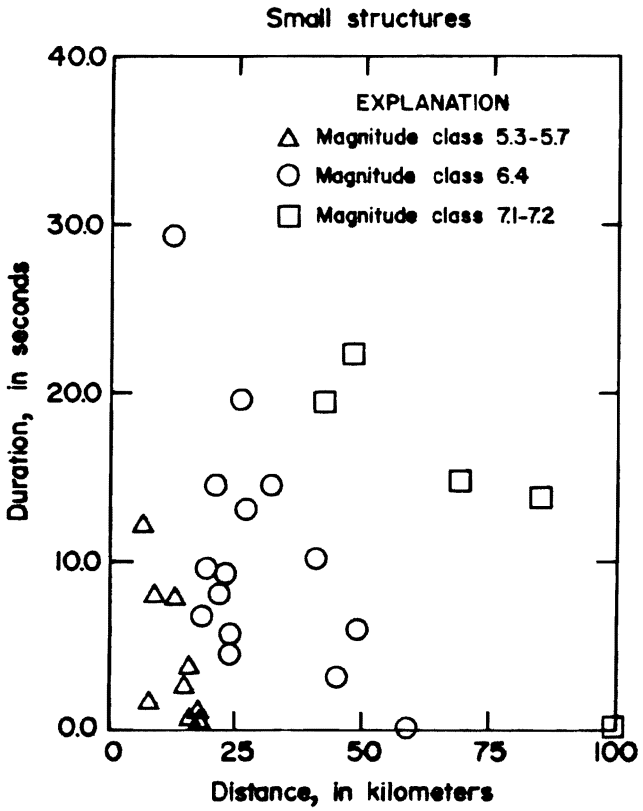

Figure 14. Duration versus distance from slipped fault for recordings from small structures (from Boore and others, 1978).

3.2.4 Response Spectrum

The following characteristics at the site are defined for a maximum possible earthquake generated from a maximum possible earthquake in the Mount St. Helens Seismic Zone:

Acceleration (horizontal)	17% g	
Velocity	25 cm/sec	(9.75 in/sec)
Displacement	10 cm	(3.9 in)
Duration	19 sec	(approximate)
Predominant period	.35 sec	(approximate)

The original design response spectrum for the Safe Shutdown Earthquake at the Trojan Nuclear Power Plant (FSAR) was based upon a horizontal base ground acceleration of 25% g. As shown in Figure 15, the effect of the maximum possible earthquake in the Mount St. Helens Seismic Zone lies inside the spectral envelope of the Safe Shutdown Earthquake as originally defined. It is therefore, accommodated by the original seismic design considerations of the facility. This is particularly true given the strong suggestions (Section 3.1.5) that a magnitude 7.2 earthquake is too conservative.

3.3 Conclusions

The Mount St. Helens Seismic Zone, a N. 20^{o} W. trending zone of moderate seismic activity extending about 100 km through the Western Cascades of Washington, consists of one or more presumed faults. Conservative analysis using a variety of available equations including the concept of seismic moment indicates a maximum possible earthquake of M = 7.2. Consideration of limited historic data suggests that a lesser quake of possibly M = 6.2 is a more reasonable maximum possible earthquake.

Assuming a 7.2 magnitude quake to be in the realm of possibility for the purpose of nuclear power plant siting, the following figures are derived for ground motion at the Trojan Nuclear Plant site: maximum horizontal acceleration - 17% g; maximum horizontal velocity - 25 cm/sec; maximum horizontal displacement - 10 cm. It is shown that the impacts of an event of this magnitude were accomodated in the original design considerations for the facility. Limited historic data suggest a very low probability (10^{-4}/year) for such an earthquake in the Mount St. Helens Seismic Zone.

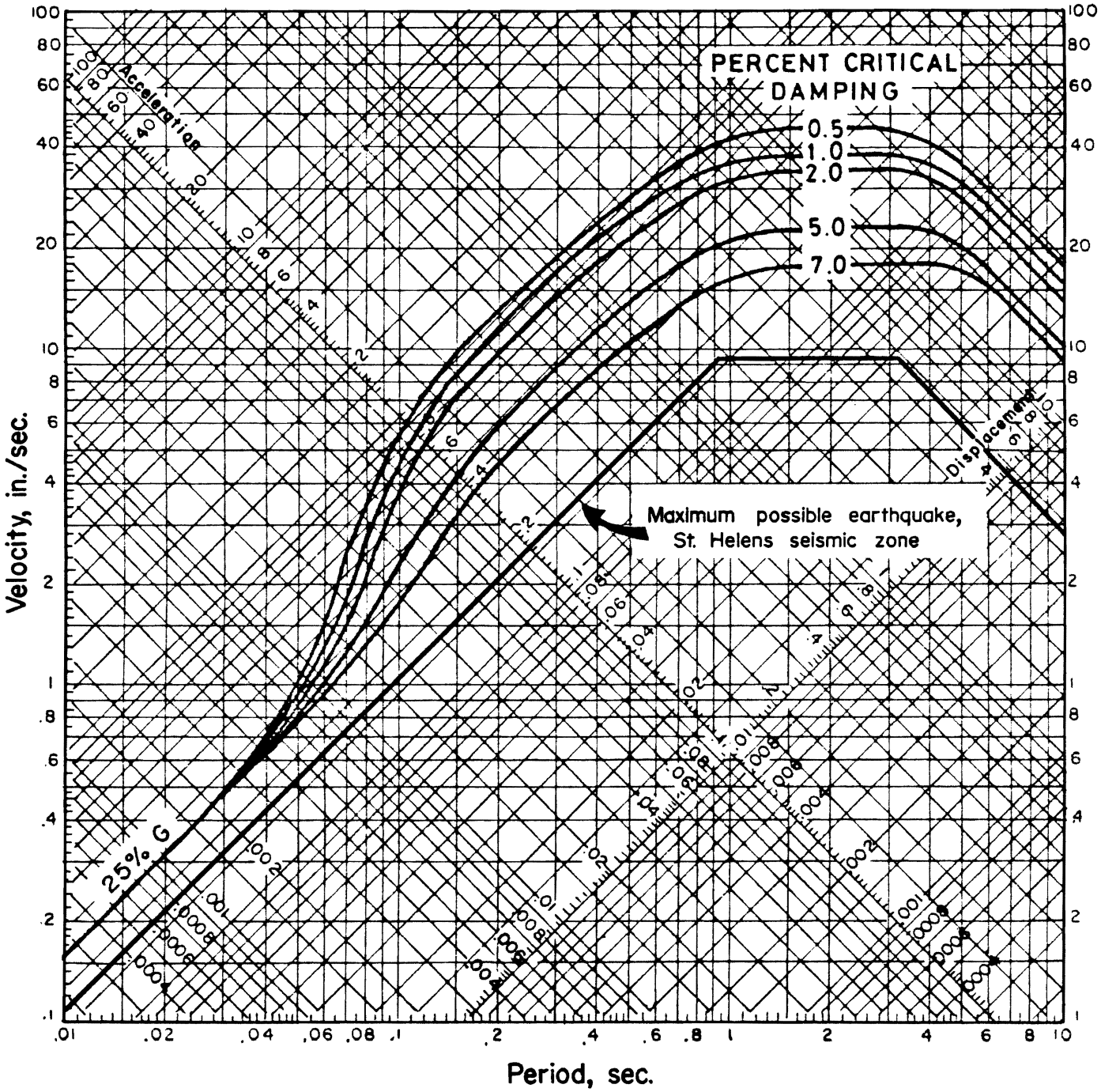

Figure 15. Design Response Spectra for safe shutdown earthquake of Trojan Nuclear Power Plant showing plot for maximum possible earthquake from St. Helens Seismic Zone.

3.4 Selected References

Applied Technology Council, National Science Foundation, Research Applied to National Needs Program, 1974, An evaluation of a response spectrum approach to seismic design of buildings: The National Bureau of Standards, Washington, D.C., 20234, Contract 3-35946.

Blume, J.A., 1965, Earthquake ground motion and engineering procedures for important installations near active faults: 3rd World Conference on Earthquake Engineering, New Zealand, v. IV, p. 53-67.

Boore, D.M., Joyner, W.B., Oliver, III, A.A., and Page, R.A., 1978, Estimation of ground motion parameters: U.S. Geological Survey Circular 795, 43 p.

---1980, Peak acceleration, velocity, and displacement from strong motion records: Seismological Society of America Bulletin, v. 70, no. 1, p. 305-321.

Brune, J.N., 1970, Tectonic stress and the spectra of seismic shear waves from earthquakes: Journal of Geophysical Research, v. 75, no. 26, p. 4997-5009.

Cloud, W.K., 1972, Strong motion earthquake records: Berkeley, California, University of California, Lecture notes, summer course.

Cloud, W.K., and Perez, V., 1969, Strong motion - Records and acceleration: Proceedings of the 4th World Conference on Earthquake Engineering, Santiago, Chile, January 13-18, 1969, v. I A-2, Impeso en Editorial Universitaria, Santiago, Chile, 1969, p. 119-132.

---1971, Unusual accelerograms recorded at Lima, Peru: Seismological Society of America Bulletin, v. 61, p. 633-640.

Coulter, H.W., Waldron, H.H., and Devine, J.F., 1973, Seismic and geologic siting considerations for nuclear facilities: Proceedings of the 5th World Conference on Earthquake Engineering, Rome, Italy, v. 2, p. 2410-2421.

Dobry, R., Idriss, I.M., and Ng, E., 1978, Duration characteristics of horizontal components of strong motion earthquake records: Seismological Society of America Bulletin, v. 68, no. 5, p. 1487-1520.

Donovan, N.C., 1972, Earthquake hazards for buildings: National Bureau of Standards Bulletin, Science Series 46, Building practices for disaster mitigation, Boulder, Colorado.

Esteva, L., 1970, Seismic risk and seismic design decisions, Seismic design for nuclear power plants, edited by R.J. Hansen: MIT Press.

Evernden, J.F., Hibbard, R.R., and Schneider, J.F., 1973, Interpretation of seismic intensity data: Seismological Society of America Bulletin, v. 63, no. 2, p. 399-422.

Gutenberg, B., and Richter, C.F., 1956, Earthquake magnitude, intensity, energy, and acceleration: Seismological Society of America Bulletin, v. 46, p. 105-145.

Hershberger, J., 1956, A comparison of earthquake acceleration with intensity ratings: Seismological Society of America Bulletin, v. 46, no. 4, p. 317-330.

Housner, G.W., 1965, Intensity of earthquake ground shaking near the causative fault: Proceedings of the 3rd World Conference on Earthquake Engineering, New Zealand, v. 1, p. III - 94-115.

---1970, Engineering estimates of ground shaking and maximum earthquake magnitude: Proceedings of the 4th World Conference on Earthquake Engineering, Santiago de Chile, v. 1, p. 1-13.

Idriss, I.M., 1978, Characteristics of earthquake ground motions, in Earthquake engineering and soil dynamics, v. III: ASCE Geothechnical Engineering Division, p. 1151-1265.

Johnson, J.A., 1978, Magnitude-dependent near source ground motion spectra, in Earthquake engineering and soil dynamics, v. I: ASCE Geotechnical Engineering Division, p. 530-539.

Joyner, W.B., Boore, D.M., Porcella, R.L., 1981, Horizontal acceleration and velocity fron strong-motion records including records from the 1979 Imperial Valley, California, earthquake: U.S. Geological Survey Open-File Report 81-365, 46 p.

Mohraz, B., 1976, A study of earthquake response spectra for different geological conditions: Seismological Society of America Bulletin, v. 66, no. 5, June 1976, p. 915-936.

Milne, W.G., and Davenport, A.G., 1969, Distribution of earthquake risk in Canada: Seismological Society of America Bulletin, v. 59, p. 754-779.

Molnar, P., 1979, Earthquake recurrence intervals and plate tectonics: Seismological Society of America Bulletin, v. 69, no. 1, p. 115-134.

Newmark, N.M., and Hall, W.J., 1969, Seismic design criteria for nuclear reactor facilities: Proceedings of the 5th World Conference on Earthquake Engineering, Santiago, Chile, 1967, v. 2, p. 37-50.

Newmark, N.M., and Rosenblueth, E., 1971, Fundamentals of earthquake engineering: Englewood Cliffs, New Jersey, Prentice-Hall.

Page, R.A., and others, 1972, Ground motion values for use in the seismic design of the Trans-Alaska pipeline system: U.S. Geological Survey Circular 672.

Portland General Electric Company, 1976, Final safety analysis report - Trojan Nuclear Plant: Portland General Electric Company Docket 50-344, v. 1, v. 2.

Sauter, F.F., 1979, Damage prediction for earthquake insurance: Proceedings of the 2nd U.S. National Conference on Earthquake Engineering, Aug. 22-24, Stanford University, p. 90-108.

Schnabel, P.B., and Seed, H.B., 1973, Accelerations in rock for earthquakes in the western United States: Seismological Society of America Bulletin, v. 63, no. 2, p. 501-506.

Seed, H.B., 1975, Earthquake effects on soil-foundations systems, in Winterkorn, H.F., and Fang, H., eds., Foundation engineering handbook: New York, N.Y., Van Nostrand Reinhold Company, p. 700-732.

Seed, H.B., and Idriss, I.M., 1970, Soil moduli and damping factors for dynamic response: Berkeley, Calif., University of California Report No. EERC 70-10, Earthquake Engineering Research Center.

Seed, H.B., Ugas, C., and Lysmer, J., 1976, Site dependent spectra for earthquake resistant design: Seismological Society of America Bulletin, v. 66, no. 1, p. 221-243.

Shannon and Wilson, Inc., 1974, Geotechnical investigation for central plant facilities, Pebble Springs site, Boardman nuclear project, Gilliam County, Oregon, v. 1, Summary report, Appendix B, Earthquake and ground response analyses.

Stacey, F.D., 1969, Physics of the earth: New York, John Wiley and Sons, Inc., 324 p.

Trifunac, M.D., 1976, Preliminary analysis of the peaks of strong earthquake ground motion - Dependence of peaks on earthquake magnitude, epicentral distance, and recording site conditions: Seismological Society of America Bulletin, v. 66, no. 1, p. 189-219.

Trifunac, M.D., and Brady, A.G., 1975, On the correlation of peak acceleration of strong motion, with earthquake magnitude, epicentral distance, and site conditions, in Proceedings of United States National Conference on Earthquake Engineering, 1975, Ann Arbor, Mich., p. 43-52.

---1975, On the correlation of seismic intensity scales with peaks of recorded strong ground motion: Seismological Society of America Bulletin, v. 65, no. 1, p. 139-162.

Woods, R.D., 1978, Measurement of dynamic soil properties, in Earthquake engineering and soil dynamics, v. 1: ASCE Geotechnical Engineering Division, p. 91-178.

Woodward-Clyde and Associates, 1970, Ground motions, Trojan nuclear plant, Rainier, Oregon: Report to Bechtel Corporation, 5 p., 2 tables, 3 figs.

4.0 VOLCANIC EVALUATION OF MOUNT ST. HELENS RELATIVE TO TROJAN SITE

4.1 Introduction

4.1.1 General

Mount St. Helens is a relatively young volcanic cone in the Cascade Range of Washington. The general geology is characterized by dacite domes, pyroclastic flows, lahars, mudflows, and tephra with the last 4500 years well documented by Crandell and Mullineaux (1978) and the earlier 35,000 years documented in more general form by Crandell and Mullineaux (1973) and Hyde (1975). Minor flows of basalt and andesite are noted within the past few thousand years.

Volcanic hazards evaluated in this survey include ash fall, pyroclastic flows, mudflows, floods, and lateral blasts. The evaluations are based on existing published and unpublished data and are designed to identify the maximum credible event for each type of hazard under consideration. With the exception of domes and local flows of basaltic and andesitic lava on the vent, lava flows are rare. Basaltic flows extend a maximum of only 15 km south of the vent to the vicinity of the Lewis River. As noted previously (Section 1.0) they warrant no further consideration in this investigation.

Assessment of volcanic events at Mount St. Helens and their possible relationship to the Trojan Nuclear Plant differs from that of seismic events owing to the more general guidelines and to the greater difficulty of quantifying volcanic events as compared to seismic events.

The procedure adopted here is aimed clearly at placing bounds on the maximum credible volcanic events at Mount St. Helens that may impact Trojan. A maximum credible event is the greatest event of a given type that can reasonably be expected to occur given the geologic stage of development of the volcano. This approach is analogous to that applied to the analysis of earthquakes in the sense that conclusions proceed from our knowledge of the actual geologic feature in question.

4.1.2 Precursors

Precursors to volcanic eruptions include seismic activity, tilting, ground deformation, gas emissions, bulging and others. On a broad scale, the actual geology of the vent and the surrounding area provides a general measure of the potential for eruptions in the foreseeable future.

Experience shows that in general terms the size of a volcanic event is proportional to the size of the precursors. Thus, daily or weekly eruptive events at Mount St. Helens, for example, are preceded by small events incapable of detection without use of sensitive equipment. Larger events are preceded by larger precursors. The May 18, 1980 eruption was preceded by two months of seismicity and other precursors including several hundred feet of bulging on the north side.

On a larger scale, truly catastrophic events which greatly modify the geology of a volcanic vent are preceded by geologic indications of large magma chambers. The geology of a vent, then, is indicative in a very general way of the capability of the vent. Interpretations of maximum credible events can be based on this geology and are valid until that geology changes or our knowledge of the geology is significantly revised.

As a general rule, the largest possible future event that will occur in the foreseeable future (until the geology actually changes) will not exceed the largest known event in the history of the mountain. To apply this maxim, two conditions must be met. First, the geologic record must be fairly complete and it must be well understood. Second, subsidiary vents, faults, and other volcanic features must not suggest that the volcano in question is only a small part of a greater volcanic system. At Mount St. Helens, both conditions are met. Use of the geologic record to bound maximum credible events is, therefore, valid.

4.1.3 Maximum Credible Events

The concept of maximum credible event places finite real limits on hazard interpretations that otherwise have no rational bounds. Statistical projections, for example, must be limited by credible events in the realm of volcanic activity in much the same manner that measurements of fault source parameters place limits on possible earthquakes. The limits in both cases are dictated by the very geologic nature of the actual feature under investigation.

At the risk of overemphasis an additional example is instructive. If a person climbs stairs at the rate of one flight every 10 seconds, we can conclude he can climb 60 flights in 10 minutes. If we now limit his activity to the State Office Building in Portland, however, he can climb no higher than 10 flights regardless of the time we give him. A specific feature, in this case the State Office Building, defines a maximum credible event in this scenario and places a limit on our projections.

Likewise, our knowledge of a specific volcanic feature, in this case Mount St. Helens, places real limits on our projections of future activity. In a very real sense we can say that events larger than responsibly defined maximum credible events have a probability approaching zero.

In this approach a reasonably complete understanding of the volcano is required and in the case of Mount St. Helens, this knowledge is available. In this approach, the magnitude of prior events is examined using a variety of sources and time frames from the geologic to the historic.

Ideally this approach would address a complete record of past events in both human and geologic time frames as a means of postulating a maximum credible event for each hazard. Where research is incomplete, or data are lacking, conceptualizing a maximum credible event is less certain. Here it is necessary to view conclusions with subsidiary techniques. A conservative approach is needed to accommodate the uncertainties of these less direct methods of analysis.

It is clearly not rational to direct an investigation of this sort at volcanoes other than the one under investigation unless the knowledge so gained is intended generally for supplemental understanding. Appropriate comparisons with similar volcanoes, or the results of ongoing research are factored into the analysis to more precisely place limits on possible events. Equating Mount St. Helens with Crater Lake, for example, is not valid any more than is equating the Mount St. Helens Seismic Zone with the San Andreas Fault.

4.2 Lateral Blast (Violent Nuée Ardente)

Lateral blast (violent nuée ardente) is the forceful directed release of volcanic material laterally from the sides of a volcano. The violence of the eruption results either from the buildup of pressure beneath an obstruction to the release of gas on the volcano or in some instances to a postulated very rapid generation of volatiles and gas too immense to be accommodated by an open pre-existing vent. The effects of lateral blasts by their nature are not fully preserved in the geologic record and therefore are more difficult to interpret in terms of maximum credible events for a given vent.

Lateral blasts at Mount St. Helens were not included in the FSAR for the Trojan facility (Portland General Electric Company, 1976); Crandell and Mullineaux (1978) postulated possible lateral blasts extending 10 km from Mount St. Helens. The lateral blast of May 18, 1980 resulted in complete devastation for distances of up to 20 km, and sear zones up to 25 km from Mount St. Helens.

Examining the last 1,500 years activity of the volcano, Hoblitt and others (1980) record that a lateral blast approximately 1,000 B.P. scattered rock debris a distance of 6 km or more northeastward from Sugar Bowl, a dome located 1,000 feet lower than Goat Rock on the northwest side of the volcano. The blast was associated with the emerging dome and was associated with little ash. It was minor in comparison with the blast of May 18, 1980.

A lateral blast eruption at Bezymianny volcano in Kamchatka in 1956 is described by Tazieff (1961) as "perhaps the most violent eruption of the Twentieth Century". The size and pattern of the eruption are so nearly like the May 18 Mount St. Helens event that a comparison is instructive. At both, small earthquake swarms preceded small phreatic ash eruptions that opened small craters at the summit. The upper flanks also were severely deformed by rising magma as the minor phreatic eruptions continued to enlarge the summit craters. Elevation and lateral movement of large volumes of the upper flanks reached more than 300 feet and the slopes steepened accordingly. Strong earthquakes triggered huge landslides and paroxysmal eruptions at both sites. Large fan shaped areas were devastated at both; 193 mi^2 at Bezymianny and 190 mi^2 at Mount St. Helens. The lateral blasts at both were followed by violent vertical eruptions that spewed ash to great elevations to be distributed by the prevailing winds. Both mountains lost 600 to 1,200 ft of their tops and developed amphitheater shaped craters roughly 1 mile to 1½ miles in diameter.

At Bezymianny soon after the March eruption the last phase of the huge eruption began as a viscous dome began to build, and by November 1956 as the eruptive cycle appeared to end had grown to a mass 2,400 ft in diameter and 1,050 ft high. Intermittent eruptive activity has continued at Bezymianny and there was another major eruption in 1979.

From a review of lateral blast type eruptions in the literature including the May 18, 1980 Mount St. Helens eruption, it appears that they generally occur early in an eruptive cycle. In general terms, the lateral blast of May 18, 1980 was caused by a sudden unroofing of a volatile-rich geothermal system within the vent. This was preceded by magmatic activity, an earthquake, and catastrophic landslide. Although the landslide was the immediate trigger, it is clear that the driving mechanism was the broader eruptive activity which began in late March of 1980 or earlier.

The term "lateral blast" is rejected by Kienle (1980) in terms of the actual eruption and is applied by him instead to the complex barometric phenomena resulting from the eruption. This refinement is not adopted here. As a further clarification it is emphasized that examination of the semantics of the term "lateral blast" does not constitute a rejection of the concept of a violent lateral eruption.

Although the lateral blast at Mount St. Helens was associated with an ash eruption, the violence of a given lateral blast does not necessarily correlate with the volume of the ash. Further, lateral blasts at Mount St. Helens appear in a general way to be more closely related to dome formation. In the Sugar Bowl (1,000 years B.P.) and Goat Rocks (1980) events the most recent active dome was the site of the blast. One can possibly envisage a pocket of gas exsolving from cooling magma in the vent under the dome over a period of time. Because lateral blasts are controlled by the overburden above the gas, they are directed radially from the parent dome away from the volcano. A geologic map of Mount St. Helens (Hopson, 1980; Crandell, 1978) shows that there are domes located at the summit and on all sides of Mount St. Helens except for the due south quadrant. Pyroclastic flow deposits are also present on most of the drainages surrounding the volcano. Large explosive eruptions could take place at the site of any of these domes sometime in the life of the volcano, although this is not likely in the present eruptive cycle.

The lateral blast of May 18, 1980 removed 1 mi^3 of the summit of the volcano and probably was an event unexcelled in the history of the volcano. Oriented toward Trojan 55 km distant (maximum impact 25 km distant), it would have had no impact on that facility.

According to Kieffer (1980) a near surface magma reservoir 0.12 km^3 in size and constrained by 650 meters of overburden was involved in the 1980 event. As noted above these physical conditions will not be duplicated in the present eruptive cycle, at least not without significant diagnostic precursor activity, none of which is observed at the present time. The distance (50-55 km) to Trojan from Mount St. Helens and the direction (S. 72^o W.) relative to the present configuration of the cone effectively preclude lateral blast as a serious consideration to the Trojan site.

4.3 Ash Fall

Ash fall is the accumulation of airborne fine-grained volcanic debris ejected in a volcanic eruption. Because of their wide distribution over a variety of landforms, ash falls are well preserved in the geologic record. The geologic record then can provide a reliable measure of maximum credible events for a volcano, if the geologic record is adequately defined. Further, knowledge of the volcanoes of the world shows a complexity of intensity, periodicity, and character of ash eruptions between vents that precludes direct comparison of one vent directly with another with the intent of developing final conclusions. Statistical studies of populations of geologically similar vents can provide an added dimension to hazards analysis, but are beyond the scope of this investigation.

At Mount St. Helens detailed studies prior to the May 18, 1980 eruption (Crandell and Mullineaux, 1978; Hopson, 1971; Hyde, 1975; and Hoblitt, 1980) provide us with a fairly complete knowledge of the total eruptive history of the volcano and allow a reasonable and accurate assessment of the maximum credible ash fall.

Previous ash eruptions at Mount St. Helens have involved a wide range of estimated volumes including 0.01 km^3 in 1842, 0.1 km^3 in 1800 (Layer T), 1 km^3 4,000 years B.P. (Layer Yn) (Crandell and Mullineaux, 1978), 10 km^3 for all

Y sets and 1-2 km^3 for set P (Crandell and Mullineaux, 1973). These crude figures of a logarithmic nature are general and subject to refinement. Kienle (1980) estimates equivalent magma volumes of 0.4 km^3 and 2.4 km^3 for layers T and Yn, respectively. In addition, he calculates a magma equivalent volume of 1.7 km^3 for Layer Wn (350-450 y B.P.). Using isomass calculations, which are probably more conservative and more accurate than some of the techniques employed above, Sarna-Wojicki (1980) calculates a magma mass equivalent of 0.14 km^3 for the May 18, 1980 ash eruption. Kienle (1980) estimates a volume of 0.20 km^3.

Large ash falls are restricted to the north, east, and south and include maximum measured thickness in the past 4,500 years near the vent of 50 cm (1800 A.D., T Layer), 150 cm (1500 A.D., W Layer), 30 cm (500 A.D.-500 B.C., B Layer), and 70 cm (1000 B.C., P Layer), according to Crandell and Mullineaux (1978). Maximum thickness of 100-200 cm on the north and east flanks of the vent are reported for Layer Y (1750-2500 B.P.) by Hoblitt (1980). For Layer W (350-450 B.P.) Hoblitt (1980) reports seven beds with maximum thicknesses of 1 m at 10 km and 8 cm at 80 km for the lowermost (Wn) ash-fall unit. Along an axis of maximum deposition the largest eruption (Yn) deposited an estimated 60 cm of ash at a distance of 50 km from the vent (Crandell and Mullineaux, 1980; Figure 9). This figure is consistent with other stated data for the ash fall.

We know of no reported occurrence of volcanic ash of Mount St. Helens origin in the geologic record in the vicinity of the Trojan site. Small accumulations of a few millimeters thickness, such as those of the present eruptive cycle, may escape detection in the geologic record.

The Yn event (probably several cubic kilometers) is generally accepted as the greatest ash eruption to be emitted in the life of the volcano extending back perhaps as far as 40,000 years. The large pre-4500 B.P. ash events are noted by Hyde (1975) and include the event (35,000-40,000 B.P.) which may be present in the silt of the Willamette Valley, Oregon (Newhall, 1981, oral communication). At the type section of the Willamette Silt (mid-Willamette Valley), Glenn (1965) notes a 0.5 inch thick layer of ash. It is approximately at the appropriate stratigraphic position.

By comparison, the May 18, 1980 event deposited 4.5 cm of ash at a rate of 1.3 cm per hour at Packwood, Washington along the axis of maximum deposition

and equidistant from Mount St. Helens as Trojan (50 km). The tephra was blown rapidly to the northeast across Washington and Idaho in a relatively narrow plume and reached western Montana 600 km (360 miles) in less than 11 hours. The ash layer thinned rapidly away from the volcano and also with distance from the axis of the lobe. Some anomalous thickness vs. distance patterns are present because wind patterns or agglutination of ash particles caused more rapid deposition in the area near Ritzville, Washington.

Assuming the Yn event to be the worst credible event that can be expected from the volcano, it can be shown that a maximum credible event along the axis of maximum accumulation is 60 cm of ash at a distance of 50 km from the vent. There has been one such eruption in the past 4,500 years, and it is doubtful that any events of similar magnitude have occurred in the 40,000 year history of the mountain.

Maximum credible ash fall at Trojan from Mount St. Helens is a function of volume of ash erupted and direction of transport. An additional consideration during the present eruptive cycle is the limitations that the existing open conduit may place on the occurrence of a large eruption. A maximum credible ash eruption will occur once every 40,000 years. The existence of an active eruptive cycle limits the chance of large eruption in the short term, in the sense that an open vent is now available to release volatiles. It does not, however, rule out the possibility of a large eruption entirely. Some prior eruptions (Kalama, 350-450 B.P.; and Goat Rocks, 1800) follow dacite-andesite-dacite patterns and demonstrate a measure of disorder and lack of predictability in the large-scale sequence of behavior of the volcano. Thus, from a conservative standpoint the timing between events may also exhibit disorder. We can, therefore, place limits on the size of maximum credible events, but in an absolute sense we cannot do so with the timing. The existence of an active vent may reduce the chances of a maximum credible event by a factor of 10 to 1 during the present eruptive cycle.

Statistically, winds flow from Mount St. Helens toward Trojan 1 percent of the time. The five largest ash falls in the last 4,500 years of the life of the volcano follow the statistically favored wind directions to the north and the east (Crandell and Mullineaux, 1978). As noted previously, a thin layer of ash possibly originating from a much older ash eruption on Mount St. Helens according to recent interpretations is reported in the Willamette Valley (Glenn, 1965).

The approximate chances of a maximum credible ash event may be on the order of 1 chance per year in 4×10^6 or 4×10^7 (1/40,000 x 1/100 x 1/10). Lesser ash falls of greater chance might also be of concern to the safe management of the plant. Using the data of Crandell and Mullineaux (1978) it can be shown that an 8 cm event at Trojan may have a probability of 1 chance in 5×10^5 to 10^6 years. In both cases precursors would precede the event.

It is concluded in general terms that a maximum credible ash fall will be equivalent to the Yn Layer, 4,500 years ago (60 cm at 30 miles) and that the plume will be directed in the direction of statistically favored wind flow. The geologic record and the statistical spread of wind direction to the east support this. The probability that a maximum credible eruption could be directed toward the Trojan site is very slight, especially in the present eruptive cycle. Lesser eruptions of higher probability could also impact the site but would be more manageable and would be preceded by significant precursor activity.

4.4 Pyroclastic Flows

4.4.1 General

Masses of hot dry rock fragments mixed with hot gases traveling downslope as though they were fluid are called pyroclastic flows. They owe their mobility to gravity and to the explosive force of the eruption and their expanding gases. They are formed by the conversion of rock material to ash size particles by the rapid discharge of gas. The expanding cloud then assimilates and transports blocks, boulders, and smaller fragments in a highly heated but not fused state, downslope. Pyroclastic flows can form in several ways. Large pyroclastic flows can form from an explosive eruption at an open vent as parts of the eruption column fall back onto the flanks. They are characterized by flow downslope guided somewhat by the topography. Explosive activity at the base of a dome can expel moderate to large amounts of pumice and gas charged fragments laterally. Thirdly, portions of a steep sided building dome may collapse to send a mass of incandescent rock and finer debris cascading or exploding to lower elevations.

At one end of the spectrum pyroclastic flows are hot products of concurrent volcanism which may have associated with them hot clouds of volcanic ash and debris. At the other end of the spectrum mudflows (Section 4.5) located farther from the vent are possible if large volumes of water are incorporated in the mass from melting snow, ice, or pre-existing rivers. Pyroclastic flows and mudflows are well preserved in the geologic record and a consideration of that record provides a good measure of maximum credible events.

4.4.2 Potential for Pyroclastic Flows

Pyroclastic flows, owing their mobility to gravity and to expanding volcanic gases, are characterized by high temperatures, and high velocities between 50 and 150 km per hour. Hazards may extend up to 10 km or more from the vent as seen historically at Mt. Pelee, Mt. Vesuvius, Mt. Katmai, and Mount St. Helens. For Mount St. Helens, pyroclastic flows are well preserved in the geologic record and are well studied in the literature (Crandell and Mullineaux, 1973; Hyde, 1975; Crandell and Mullineaux, 1978; and Hoblitt, 1980). Consideration of the known geologic record of pyroclastic flows at Mount St. Helens (Table 10) provides a good basis for assessing future events.

Prior to the May 18, 1980 eruption. Crandell and Mullineaux (1978) predicted that nearly all areas within 6 km of the base of the volcano could be impacted by future pyroclastic flows, and that locations within 10 km of the base in major drainages could be impacted. Incorporation of water in the flow could generate mudflows at greater distances as discussed here in Section 4.4.3.

The May 18, 1980 eruption and later eruptions at Mount St. Helens produced many pyroclastic flows primarily through partial collapse of the erupting ash column. Most were channeled to the north by the shape of the vent area. The initial eruption was a combination of lateral blast and pyroclastic flow and devastated a large area north of the cone (Section 4.2).

The present configuration and eruptive phase of the volcano indicate that small to moderate pyroclastic flows may occur and that they will be directed to the north. A maximum credible event exclusive of lateral blast could extend 10 km down major drainages, but probably will not occur in the present eruptive cycle. Greater extents are possible if pyroclastic material incorporates large amounts of water. This type of phenomenon is discussed under mudflows below (Section 4.4.3).

Table 10

Extent of pyroclastic flows and mudflows
from Mount St. Helens in past 4500 years
(Adapted from Crandell and Mullineaux, 1978)

Year	Mudflow			Pyroclastic Flow		
	NW + N	SE + E	S + SW	N + NW	E + SE	S + SW
2000	≥ 3 km ≥ 9 km ≥ 3 km	≥ 9 km	≥ 4 km	≥ 5 km		9 km
1000					≥ 3.5 km	
0		≥ 18 km	≥ 30 km (Swift) ≥ 45 km (Kalama)	≥ 4 km	≥ 13 km	8 km
-1000	≥ 70 km (Toutle)	≥ 15 km			≥ 11 km	
-2000				≥ 30 km (Mudflow?)	≥ 4 km	

4.5 Mudflows

4.5.1 General

When significant volumes of water become incorporated into moving volcanic material, a mudflow is generated. Mudflows may originate from: (1) the release of water from a crater lake, (2) rapid melting of snow or ice under extensive pyroclastic flows, (3) explosive introduction of volcanic material into bodies of standing water, (4) descent of pyroclastic flows into river channels, or (5) collapse of an unstable volcanic cone resulting in a saturated avalanche or introduction of the collapsing material into water bodies downslope. Speeds depend on slope and water content and may approach 30 to 50 km per hour. At Cotopaxi volcano in Equador, velocities of 80 km per hour were achieved. At Bezymianny, mudflows traveled a distance of 80 km beyond the base of the volcano in 1956.

During the 4,500 year recent history of Mount St. Helens, pyroclastic flows and mudflows have occurred on all flanks of the volcano (Table 10). Maximum extents include 30 km down the Swift Creek - Lewis drainage, 70 km down the Toutle and Cowlitz, and 45 km down the Kalama. In the preceding eruptive period (4,500 to 40,000 years ago) the maximum event to the south of the volcano extended 24 km down the Lewis River (Hyde, 1975) to Woodland (Newhall, oral communication, 1981). Volume estimates of these pyroclastic flows are not possible, although general geographic distributions are well established (Crandell and Mullineaux, 1978).

The Mount St. Helens mudflows have generally involved introduction of volcanic material onto snow covered slopes or into river channels. The influence of crater lakes has been minimal, although more distant lakes such as Coldwater Lake may be a concern (see Flooding, Section 4.5). In violent eruptions such as that of May 18, 1980, Spirit Lake may have contributed water to mudflows down the Toutle River.

A final type of mudflow in need of clarification is that of a large landslide originating on the flanks of the volcano in a manner not necessarily related to volcanism on Mount St. Helens. This type of event poses only a minor threat given the small size of the volcano, the relative lack of altered material on the volcano (Crandell and Mullineaux, 1978), and the removal of much of the summit in the May 18, 1980 eruption.

Thus, the major causes of mudflow at Mount St. Helens in need of investigation are the introduction of pyroclastic material into rivers or lakes and the descent of pyroclastic flows onto snow or ice covered slopes.

4.5.2 Stream Channel Mudflows

The May 18, 1980 eruption sent pyroclastic flows and mudflows down the Toutle River and Cowlitz River toward the Columbia River. Preliminary estimates of the volume are listed as: North Fork Toutle River below Baker Camp, 157 million m^3; Cowlitz River, 61 million m^3; Columbia River, 42 million m^3 for a total of 260 million m^3 or 340 million $yards^3$. Adding the Swift Reservoir and South Fork Toutle River volumes of 18 million m^3 each, the total volumes are about 300 million m^3 or 390 million $yards^3$ (Foundation Sciences, 1980). Actual volumes of dredged material would provide a lower limit to total volume of the mudflow, but are not readily available. However, the 57 million $yards^3$ dredged from the Cowlitz River between June 1, 1980 and May 31, 1981 (Temko, written communication, 1981) is generally consistent with the above estimate for the Cowlitz River.

Debris mobilized in the upper reaches of the South Fork Toutle River traveled 45 km in 90 minutes to deliver a 12-foot wall of saturated debris to the confluence with the North Fork Toutle River. The North Fork Toutle mudflow crested much higher than the South Fork mudflow and arrived at the mouth of the Toutle with a homogeneous mortar-like consistency from bank to bank. High watermarks on the northeast arm of Spirit Lake to the east indicate that much of the water was temporarily displaced by the debris avalanche and suggests that possibly much of the water in the mudflow was derived from Spirit Lake. Alternatively, the saturated slopes of Mount St. Helens undoubtedly provided much of the water for the mudflow.

The major mudflows generated by the debris avalanche, lateral blast deposits, and pyroclastic flow deposits of the May 18 eruption were of large volume and occurred in all the main river systems except that of the Kalama River. Immediately following the eruption, mudflows moved rapidly down Smith Creek, Muddy River, and Pine Creek and into the Swift Reservoir and in 3 hours dumped 11,000 acre feet of water, mud, and debris in the upstream area of the reservoir (Cummans, 1981). Concurrently mudflows developed in the upper reaches of the

South Fork Toutle River and traveled about 45 km in 90 minutes. In 2 hours the 12-foot wall of saturated debris reached the confluence with the North Fork and by 1:00 p.m. (5 hours) had entered the Cowlitz River. The specific gravity at Castle Rock was 2.1 with estimated flow rates of 120,000-170,000 cfs (Kienle, 1980).

The much larger North Fork Toutle mudflows took somewhat longer to develop and grew from 12:00 to 1:00 p.m. The debris avalanche and pyroclastic flow deposits formed a huge 17 mile long deposit at least 400 feet deep at the upper end near Spirit Lake and about 150 feet deep at the downstream end near Elk Rock. The flows developed along both sides of the valley initially but rapidly built up to devastate the North Fork Toutle River Valley. The North Fork mudflow in some places crested nearly 10 meters higher than the South Fork flow. The mudflow arrived at the Cowlitz River in about 8 hours where it was homogeneous and of mortar-like consistency from bank to bank. The discussion by Cummans (1981) gives details of peak flow, velocities, and time tables.

It has been shown (Portland General Electric Company, 1980) that rerouting of the location of the 1980 Toutle River pyroclastic-mudflow event down the Lewis River would yield 23 x 10^6 m^3 of sediment in the Columbia River. Routing the event down the Kalama River would yield 5 x 10^6 m^3 in the Columbia River.

The pyroclastic flow-mudflow of 2,500-3,000 years ago as mapped by Crandell and Mullineaux (1978) extended down the Toutle River and Cowlitz River to Castle Rock and included distal fluvial deposits. Conceivably it was related to the P event, but this has not been demonstrated. It also corresponds in time with an abrupt 60-foot deepening of Spirit Lake. The event in total extent was significantly larger than that of May 18, 1980. Given the complete nature of the geologic record it provides a good measure of a maximum credible event in terms of mudflow extent. It would be preceded by a wide variety of diagnostic precursors.

4.5.3 Mudflows of Pyroclastic Cloud Origin

A mudflow resulting strictly from ash cloud phenomena might in a maximum case be expected to cover 26 km^2 of snow covered terrain with 15 feet of water equivalence. This translates into 96,000 acre feet of displacement as compared to a total capacity of 756,000 acre feet for Swift Reservoir (Newhall, 1980). It is this type of scenario that Crandell and Mullineaux (1978) used in making their estimated volume 110-125 x 10^6 m^3 (100,000 acre feet). An ash cloud of comparable size spread pyroclastic material over a 30 km^3 area south of the volcano 2,500-3,500 years ago.

Pacific Power and Light Company (September 1980) evaluated the future probable events that might affect generating projects on the Lewis River, and determined that future eruptions may occur over a period of years, with little likelihood of a lateral blast to the south. The most likely event to cause problems to Swift Reservoir in the short term is a fallback type pyroclastic flow which would cause rapid melting of some or all of the remaining ice or snow pack on the mountain followed by floods or mudflows entering Swift Reservoir. A pyroclastic flow could reach the Swift Dam and powerhouse with high enough temperatures to damage unprotected electrical and control equipment. The estimate by Crandell and Mullineaux (1978) of 100,000 acre feet was based on the pre-May 18, 1980 configuration of the volcano. Now with 400 m (1,300 ft) missing from the summit area, the overall drainage area of the Swift Reservoir has been reduced by 2 km^2 0.46 mi^2. These areas were formerly those of greatest snow cover (Dunne and Leopold, 1980) and the model may no longer be valid. More refined calculations (Pacific Power and Light Company, 1980) indicate a realistic maximum volume of mudflow that could occur in the future at the Swift Reservoir to be 50,000 acre feet. The difference between their figure and that of Crandell and Mullineaux (1978) is the modified topography and assumed lesser water content of the mudflow.

By means of comparison, a mudflow of this type and volume (50,000 acre feet or 80 x 10^6 yd^3) is equivalent to approximately 20 percent of the volume of the Toutle River pyroclastic flow and associated sediments for the May 18, 1980 eruption (390 x 10^6 yd^3 or approximately 250,000 acre feet).

4.5.4 Summary

In summary, a maximum credible pyroclastic-mudflow event involves generation of pyroclastic material of volume equivalent to the Toutle event of 2,500-3,000 years ago. Included in the event is fluvial deposition of volcanic debris downstream along major river channels during and after the eruption as occurred with the event of May 18, 1980. A maximum credible pyroclastic event might also involve a mudflow component similar to that modeled by Crandell and Mullineaux (1978). Finally, these volumes of material can conceivably be routed down any channel, although the present topography of the volcano strongly favors routing down the Toutle River at least in the present eruptive cycle in the absence of precursors to the contrary. Because the event of 1980, of lesser size, impacted the channel of the Columbia River, it is evident that this maximum credible event also would impact the channel. It therefore is a consideration in terms of the cooling water intake for the Trojan Nuclear Power Plant. It would be preceded by a variety of significant precursors.

The destruction of much of the cone in the May 18, 1980 eruption will favor (i.e., 10:1) the direction of future pyroclastic flows and mudflows to the north until the volcano rebuilds its summit or until a new vent becomes activated; neither of these appear likely in the present eruptive cycle. In addition, the chance of a maximum credible event occurring within the present eruptive cycle is remote (e.g., 1 in 10) in view of the nature of this and prior ash eruptions of Mount St. Helens. For the sake of discussion one might tentatively conclude that a maximum pyroclastic eruption has one chance in 4×10^6 of occurring in any given year [1/40,000 yrs x 1/10 (topographic factor) x 1/10 (eruptive phase factor)].

An event of lesser magnitude, such as the pyroclastic flow of May 18, 1980, will occur more often and might be expected to occur once every 500 years or so, given the general data of Table 10. Applying the topographic and eruptive phase factors (both viewed by the authors as very conservative) yields an annual probability of 1 in 50,000. It was this type of event that was modeled by Portland General Electric Company (1980) and for which it was demonstrated that no flood hazard exists for Trojan given the conservative flood scenarios accommodated by the FSAR (Portland General Electric Company, 1976). No such event has occurred in the life of the vent although mudflows have extended as far as Woodland, Washington. If such an event were to occur, then siltation could impact the primary source of cooling water for Trojan (Section 4.4.4). It is not presently possible to quantify this impact.

4.6 Flooding

Flooding related to volcanic activity at Mount St. Helens can be a product of rapid snowmelt under volcanic deposits, modified streamflow during a pyroclastic eruption, postulated dam failure along Swift Creek and the Lewis River arising from mudflows and pyroclastic flows or modified infiltration rates or channel geometry. Other catastrophic floods can be postulated in the event of failure of debris dams which retain newly formed lakes such as Coldwater Lake and Castle Creek Lake. In addition, volcanic debris routed down the channels of rivers through normal fluvial processes may also be a consideration to the facility.

Floods by their nature are not amenable to complete preservation in the geologic record and must be interpreted on the basis of the historic record or hydrologic analysis. The FSAR (Portland General Electric Company, 1976) models and analyzes a wide variety of hypothetical floods and adequately demonstrates that sequential dam failures along Swift Creek and the Lewis River do not pose a threat to the facility. Further, Crandell and Mullineaux (1978) show that a maximum possible mudflow in the Swift Creek drainage is equivalent to only a fraction of the storage capacity of Swift Creek Reservoir. Pacific Power and Light Company (1980) demonstrates that a maximum possible mudflow into Swift Creek Reservoir may now be only 50,000 acre feet as opposed to the 100,000 acre feet of Crandell and Mullineaux (1978) owing in part to the greatly modified topography of the present vent (Section 4.4.2). The National River Forecast Center concludes that a dam break scenario involving dams on Swift Creek would yield a water level of 30 feet MSL at Rainier, well below the siting tolerance of the facility (Portland General Electric Company, 1980).

Foundation Sciences, describes the May 1980 mudflows of Mount St. Helens enumerating at least five surges of debris or distinct mudflows down the North Fork of the Toutle River into the Cowlitz and then the Columbia. During each surge, the Cowlitz River level was raised as far south as the Kelso-Longview, Washington area 112 river miles (180 km) from the mountain. At Rainier, Oregon the Columbia River level was raised 1.5 to 2.0 m (4.5 to 6.5 feet) during May 18 and 19, 1980.

In response to a query by the NSNRC, a Portland General Electric Company (1980) letter report presented a map showing the potential extent of mudflows

in the Lewis River and Kalama River drainages. This map shows mudflows extending to within about 8 km of the Kalama River mouth which is directly across from the Trojan Plant. The flood wave calculated to be generated by the mudflow in the Kalama drainage would be about 2 meters high at its confluence with the Columbia. The map also shows pyroclastic-mudflows entering the Swift Reservoir via Swift Creek, overtopping or causing postulated dam failure for Swift Reservoir with postulated subsequent failure of Yale and Merwin Dams. The calculated flood wave from this event would reach Woodland, Washington in about one hour and would inundate areas to a height of 11 to 12 meters MSL. This model further predicts the Lewis River flood wave to reach Rainier, Oregon in about 3 hours with a peak elevation of 11 m MSL. Neither of these flood waves would reach the design elevation of the Trojan Plant. Thus, floods generated by maximum credible mudflows or by actual dam failure in the Lewis River drainage are accommodated by the original siting criteria of the facility.

An additional kind of flooding with possible ramifications to Trojan is the failure of debris dams behind which are located newly impounded lakes within the Toutle River drainage such as Coldwater Creek Lake or Castle Creek Lake. The lake in Coldwater Creek is the largest threat. According to Dunne and Leopold (1981), storage capacity for the lake to an elevation of 2,510 feet (height of the debris dam) is 100,000 acre feet. Assuming failure with a rate of downward erosion of one foot per minute, horizontal erosion of two feet per minute, and characteristics of failure analogous to that of the Teton Dam in Idaho, a maximum discharge of 475,000 cfs will occur 100 minutes after the original breach (Dunne and Leopold,1980).

The relation used in the calculation was:

$$Q = 2.64\ HW^{1.5}$$

Q = discharge
W = width (feet)
H = height (feet) = 100 max.

The volume of water discharging from the breach was doubled to accommodate the incorporation of silt, sand and debris and was routed down the Toutle to its mouth using standard routing procedures to yield a discharge at the mouth of 500,000 cfs. This would be more than twice the discharge of the May 18, 1980 North Fork mudflow at Silver Lake and compares to a May 1980 discharge of 120,000-170,000 cfs downstream at Castle Rock, Washington on May 18, 1980.

The discharge at the mouth of the Cowlitz River downstream from the Trojan facility would be less and would be far less than the discharge (3,000,000 cfs) for which the facility is adequately designed. The significance of the event lies in the potential for silt deposition in the channel of the Columbia River. As noted by Dunne and Leopold (1980), the discharge would be twice that of the May 18, 1980 event during which siltation did occur at Trojan.

In summary, maximum credible floods arising from pyroclastic flows, mudflows, dam failures, or failure of debris dams are more than adequately accommodated by the more conservative flood scenarios of the FSAR (Portland General Electric Company, 1980). Possible siltation of the channel of the Columbia River associated with the flooding of various river channels including the Cowlitz River could conceivably impact the channel at Trojan given the experience of the May 18, 1980 eruption. Quantification of siltation is not possible here given the complexity of channel erosion in tributaries to the Columbia River and our presently incomplete understanding of potential depositional patterns in the Columbia River.

4.7 Selected References

Alpha, T.R., Moore, J.G., Morley, J.M., and Jones, D.R., 1981, Physiographic changes in Mount St. Helens, Washington showing changes in its summit crater, summer, 1980: U.S. Geological Survey Map MF-1279.

Bullard, F.M., 1962, Volcanoes of the Earth: University of Texas Press, Austin, Texas, 579 p.

Crandell, D.R., and Mullineaux, D.R., 1973, Pine Creek volcanic assemblage at Mount St. Helens, Washington: U.S. Geological Survey Bulletin 1383-A.

---1978, Potential hazards from future eruptions of Mount St. Helens Volcano, Washington: U.S. Geological Survey Bulletin 1383-C, 25 p., 2 pl., 10 figs., 3 tbls.

Crosson, R.S., Endo, E.T., Noson, L.J., and Weaver, C.S., 1980, Eruption of Mount St. Helens: Seismology: Nature, v. 285, no. 5766, p. 529-536.

Cummans, J., 1981, Mudflows resulting from the May 18, 1980 eruption of Mount St. Helens, Washington: U.S. Geological Survey Circular 850-B, 16 p.

Curtis, G.H., 1968, The stratigraphy of the ejectamenta of the 1912 eruption of Mount Katmai and Novarupta, Alaska, in Volcanology: Geological Society of America Memoir 116.

Dunne, T., and Leopold, L.B., 1980, Flood and sedimentation hazards in the Toutle and Cowlitz River systems as a result of the Mount St. Helens eruptions, 1980: unpublished report for Federal Emergency Management Administration (FEMA), 64 p.

Fairchild, L.H., and Dunne, T., 1981, Prediction of future mudflow hazard on the Toutle and Cowlitz Rivers, Washington (abs.), Meeting program with abstracts: Association of Engineering Geologists, Newer horizons in engineering geology, 24th Annual Meeting, September 27-October 2, 1981, Portland, Oregon, p. 34.

Glenn, J.L., 1965, Late Quaternary sedimentation and geologic history of the north Willamette Valley, Oregon: Oregon State University doctoral dissertation, 231 p. 47 figs., 25 tbls.

Hoblitt, R.P., Crandell, D.R., and Mullineaux, D.R., 1980, Mount St. Helens eruptive behavior during the past 1,500 years: Geology, v. 8, p. 555-592.

Hopson, C.A., 1980, Geology of Mount St. Helens area, Washington: Unpublished map.

Hyde, J.H., 1975, Upper Pleistocene pyroclastic-flow deposits and lahars south of Mount St. Helens Volcano, Washington: U.S. Geological Survey Bulletin 1383-B, p. B1-B20.

Kieffer, S.W., 1981, Blast dyamics at Mount St. Helens on 18 May 1980: Nature, v. 291, p. 568-570.

Kienle, C.F., 1980 (Oct.), Evaluation of eruptive activity at Mount St. Helens, Washington: Foundation Sciences, Inc., Portland, Oregon, 101 p.

Lombard, R.E., 1981, Channel conditions in the Lower Toutle and Cowlitz Rivers resulting from the mudflows of May 18, 1980: U.S. Geological Survey Bulletin 850-C.

Luedke, R.G., 1980, Preliminary aerial photographic interpretive map showing features related to the May 18 eruption of Mount St. Helens, Washington: U.S. Geological Survey Miscellaneous Field Studies Map MF-1254.

McDonald, G.A., 1972, Volcanoes: Prentiss-Hall, Inc., Englewood, New Jersey, 510 p.

Moen, W.S., 1977, St. Helens and Washougal mining districts of the southern Cascades of Washington: Washington Division of Mines and Geology Information Circular 60, 71 p.

Moen, W.S., McLucas, G.B., 1981, Mount St. Helens ash - properties and possible uses: Washington Department of Natural Resources, Division of Geology and Earth Resources Report of Investigations 24, 60 p.

Newhall, C.G., 1981, Probabilistic hazard assessment of Mount St. Helens (abs.), Meeting program with abstracts: Association of Engineering Geologists, Newer horizons in engineering geology, 24th Annual Meeting, September 27-October 2, 1981, Portland, Oregon, p. 47-48.

Oregon Department of Energy, 1980a, Trojan Nuclear Plant - Issues related to Mount St. Helens: unpublished report, July 14, 17 p.

---1980b, EFSC/ODOE Response to additional PSR concerns regarding potential effects of Mount St. Helens eruptions on Trojan: unpublished report, September 11, 11 p.

Pacific Power and Light Company, 1980, Study of effects of potential volcanic activity on Lewis River projects: unpublished report by Board of Consultants.

Portland General Electric Company, 1980, Additional information in response to NRC request regarding eruption of Mount St. Helens, Trojan Nuclear Plant: Portland General Electric Company Docket No. 50-344, Sept. 15, 1980, 8 p.

---1976, Final safety analysis report, Trojan Nuclear Plant: Portland General Electric Company Docket No. 50-344, v. 1, 2.

Ritchey, J.L., 1980, Divergent magmas at Crater Lake, Oregon: Products of fractional crystallization and vertical zoning in a shallow water-undersaturated chamber: Journal of Volcanology and Geothermal Research, v. 7, p. 373-386.

Rittman, A., 1962, Volcanoes and their activity: John Wiley and Sons, New York, 305 p.

Sarna - Wojcicki, 1980, Areal distribution, thickness, and volume of downwind ash from May 18, 1980 eruption of Mount St. Helens: U.S. Geological Survey Open-File Report OF-80-1078, 7 p., 8 figs.

Schuster, R.L., 1980, Effects of the Mount St. Helens eruptions on civil works and operations in the Pacific Northwest: Draft copy, 42 p., 11 figs.

Tazieff, H., 1961, The Orion book of volcanoes: New York, N.Y., The Orion Press, 102 p.

U.S. Geological Survey, 1980, Preliminary aerial photographic interpretive map showing features related to the May 18, 1980 eruption of Mount St. Helens, Washington: U.S. Geological Survey Miscellaneous Field Studies Map MF-1254.

---1980, Volcanic hazards at Mount St. Helens, November 15, 1980.

Verhoogen, J., 1937, Mount St. Helens, a recent Cascade volcano: University of California, Department of Geological Sciences Bulletin, v. 24, no. 9, p. 263-302.

Wise, W.S., 1970, Cenozoic volcanism in the Cascade Mountains of southern Washington: Washington Division of Mines and Geology Bulletin, no. 60, 45 p.

Youd, T.L., and Wilson, R.C., 1980, Stability of Toutle River blockage, Mount St. Helens hazards investigations: U.S. Geological Survey Open-File Report 80-898, 12 p., 2 figs.

Zielinski, R.A., and Sawyer, M.B., 1980, Size and shape measurements of ash particles from the May 18, 1980 eruption of Mount St. Helens: U.S. Geological Survey Open-File Report 81-114, 18 p.

5.0 CONCLUSIONS AND RECOMMENDATIONS

5.1 Seismic Hazards of Mount St. Helens Seismic Zone Relative to Trojan Site

1) The Mount St. Helens Seismic Zone, a N. 20^{o} W. trending zone of moderate seismic activity, is poorly documented from a geologic standpoint, but may be capable of an earthquake of M, M_o = 7.2, although M, M_o = 6.2 is more credible.

2) An earthquake of M, M_o = 7.2 in Mount St. Helens Seismic Zone would deliver ground motions to the Trojan site that are accommodated by the original seismic design considerations of the facility.

3) Preliminary calculations suggest that the Elk Lake earthquake (February 13, 1981) possibly should have been recorded by the maximum recording accelerograph at Trojan. A more thorough analysis of this issue is advisable even though the safety of the plant is not directly involved.

4) Future geologic investigations along the Mount St. Helens Seismic Zone will further contribute to our understanding of the feature. In the absence of large scale revisions of geologic knowledge of the study area, revisions of conclusions 1 and 2 will not be required. Periodic refinement for the purpose of public information may be desirable.

5.2 Volcanic Hazards of Mount St. Helens Relative to the Trojan Site

1) Our reasonably complete understanding of the moderate to large scale past volcanic activity of Mount St. Helens justifies use of the concept of maximum credible event in assessing future risk. This approach generally is more reasonable than a strictly quantitative approach for volcanic hazards.

2) The maximum credible lateral blast does not pose a threat to the Trojan site. Further, any significant blasts are of low probability in the present eruptive cycle and would be directed by the present crater topography to the north. Precursors of any lateral blasts will include significantly increased seismicity, deformation, and probably bulging.

3) The maximum credible ash fall could deliver 60 cm of ash to the Trojan site in a period of a few days. Such an event has not occurred at the Trojan site in the 40,000 year history of the vent and in the present eruptive cycle has an estimated yearly probability of perhaps only one chance in 4×10^6 to 4×10^7. Seismicity, deformation, and tilt precursors would precede such an event.

4) A lesser ash fall event could deliver 8 cm of ash to the Trojan site also in a period of a few days. Such an event has not occurred at Trojan in the 40,000-year history of the vent to our knowledge, and in the present eruptive cycle has an estimated probability of perhaps one chance in 5×10^5 to 10^6. Seismicity, deformation, and tilt precursors would precede such an event.

5) Pyroclastic flows will be restricted to regions within 6 km of the base of the volcano with the exception of major valleys, where maximum extents of 10-15 km are possible; the potential for large pyroclastic flows in the present eruptive cycle is small, and those that may occur will probably be directed by vent topography to the north.

6) A maximum credible mudflow would be equivalent to the Toutle River event of 3,000 years ago and would significantly exceed the event of May 18, 1980. It conceivably could be routed down any river channel, although present topography of the mountain strongly favors routing to the north. Given the fact that the May 18, 1980 event delivered sediment to the channel of Trojan, it is concluded that a maximum credible event could impact the channel at the cooling water intake facility. Such an event probably would not occur in the present eruptive cycle and would be preceded by significant seismic, deformation, and tilt precursors.

7) Maximum flooding potential arising from volcanic activity is adequately accommodated in more extreme flood scenarios presented in the original flood design considerations of the facility. A related potential impact may be concurrent sedimentation near the cooling water intake structure.

5.3 Broad Considerations

1) Implementation of the above conclusions if they are judged relevant to siting requires continued awareness of geologic research in the area, ongoing monitoring of precursor activity, and an established mechanism for transmitting relevant precursor information to appropriate persons.

2) The Department of Geology and Mineral Industries reserves the right to reconsider these conclusions when new and pertinent data are available; further, timely financing mechanisms must be available to assure timely involvement by the Department when necessary.